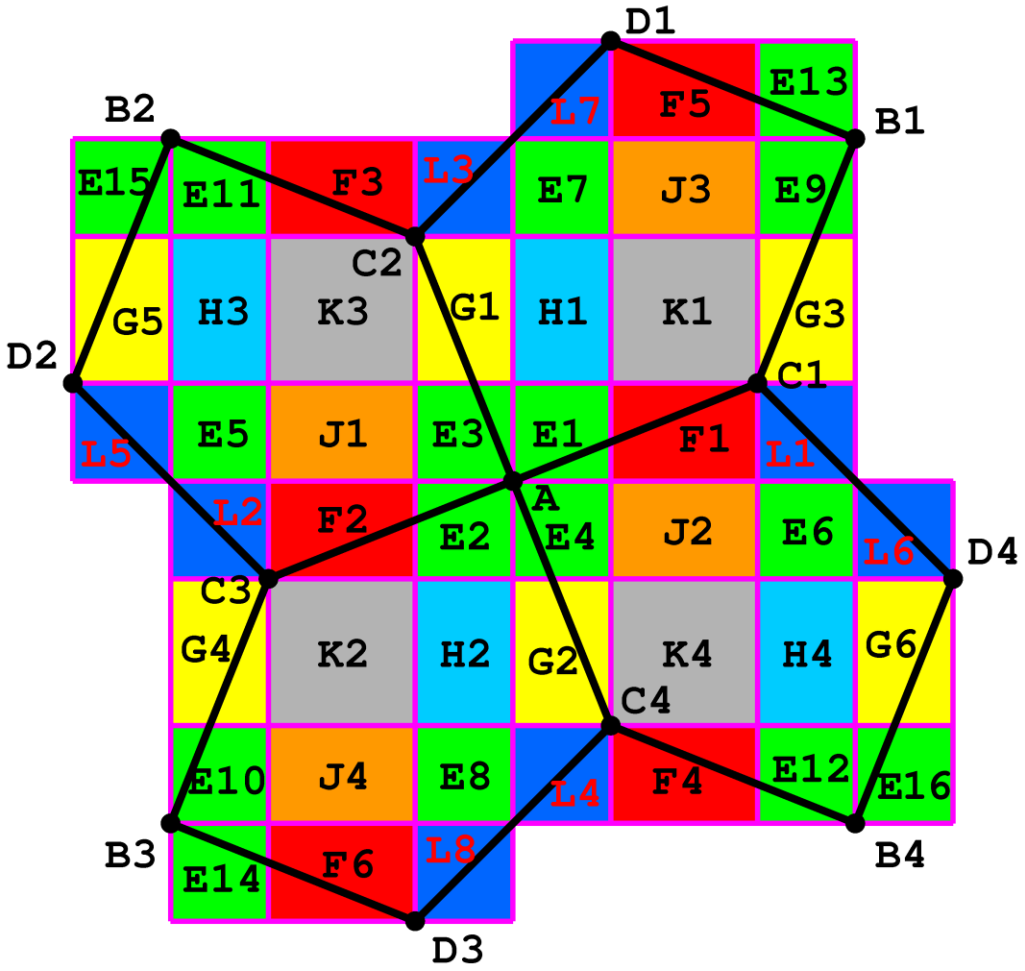


Detecting Symmetry Groups in Crystallographic Tilings

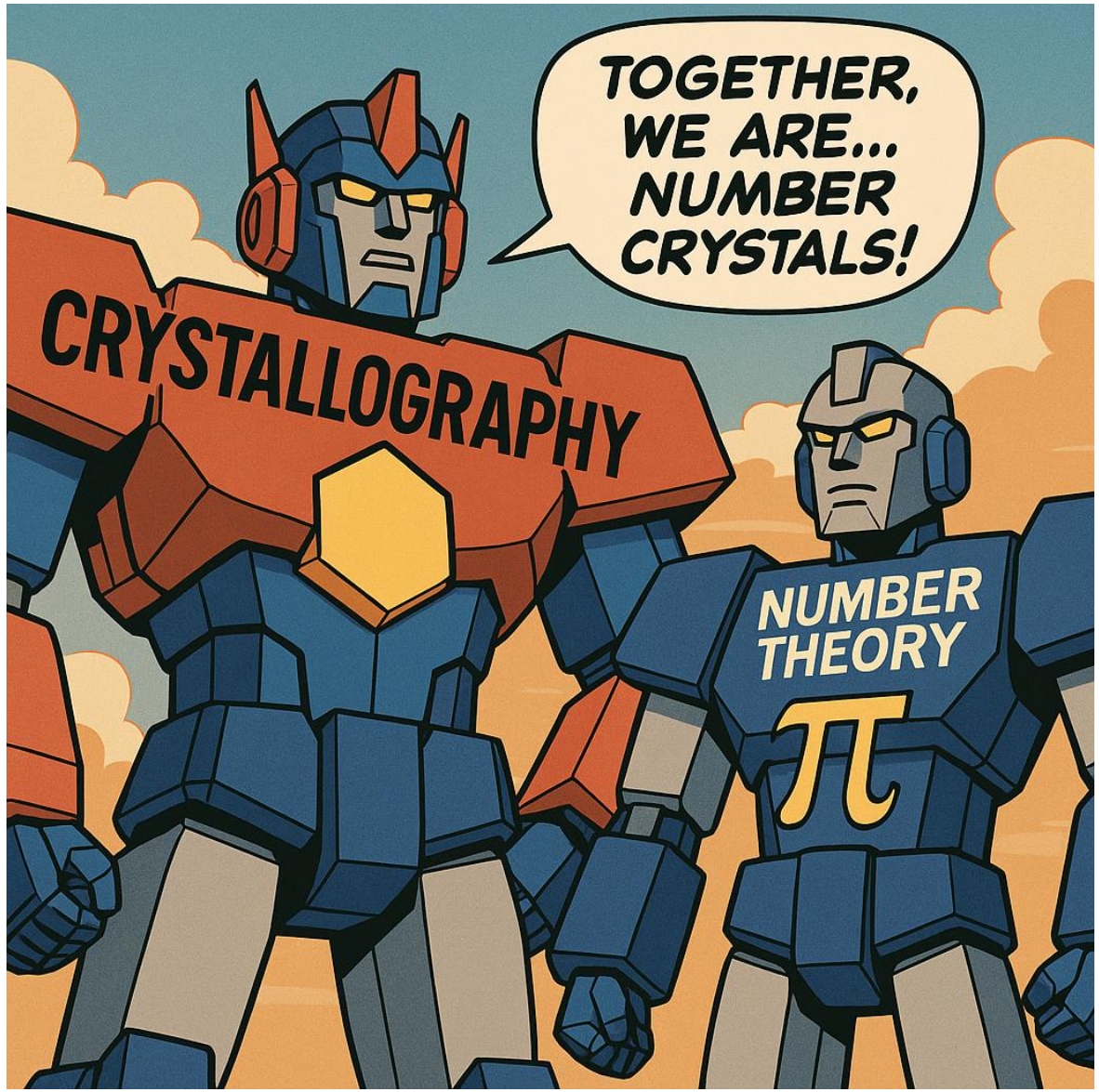
Bartosz Naskręcki

Adam Mickiewicz University Poznań

Representation Theory XIX

Dubrovnik, 26.06.2025

Why?


TOGETHER, WE ARE... NUMBER CRYSTALS!
CRYSTALLOGRAPHY
NUMBER THEORY
π





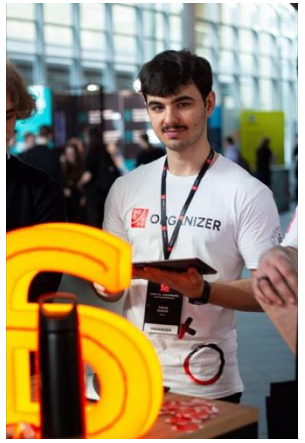






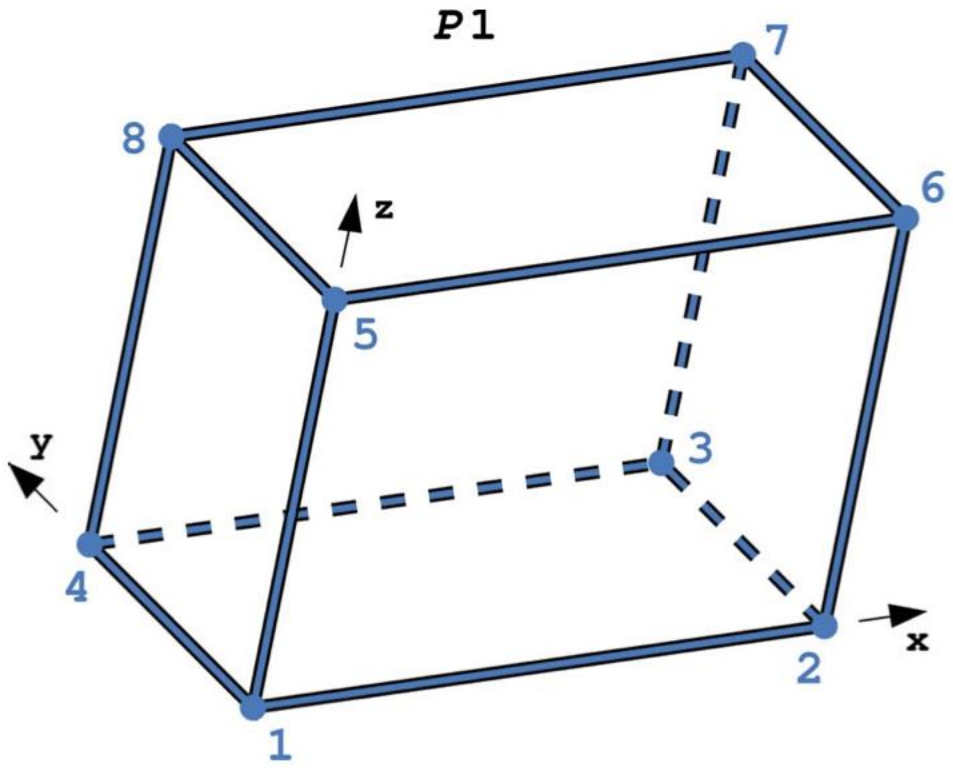


Team



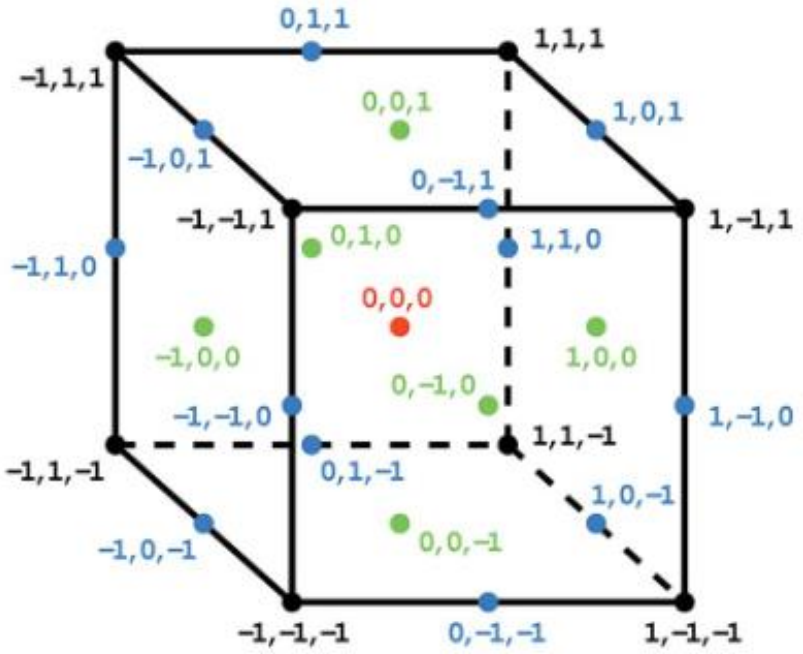


Multiplicity-weighted Euler's formula for symmetrically arranged space-filling polyhedra
Acta Cryst. A76, 317-326 (2020)



- "The applicability of the modified (normalized) Euler's formula to space-filling polyhedra with symmetrical restrictions on their bounding elements (faces, edges, vertices) is somewhat puzzling to us, structural crystallographers, who constantly utilize the concept of the asymmetric unit in our practice of structural chemistry and biology. We are curious if more qualified topologists will be able to provide a **rigorous mathematical proof** of the general correctness of this rule, so far confirmed to hold by exhaustive enumeration for all examples of crystallographic two-dimensional and three-dimensional groups."

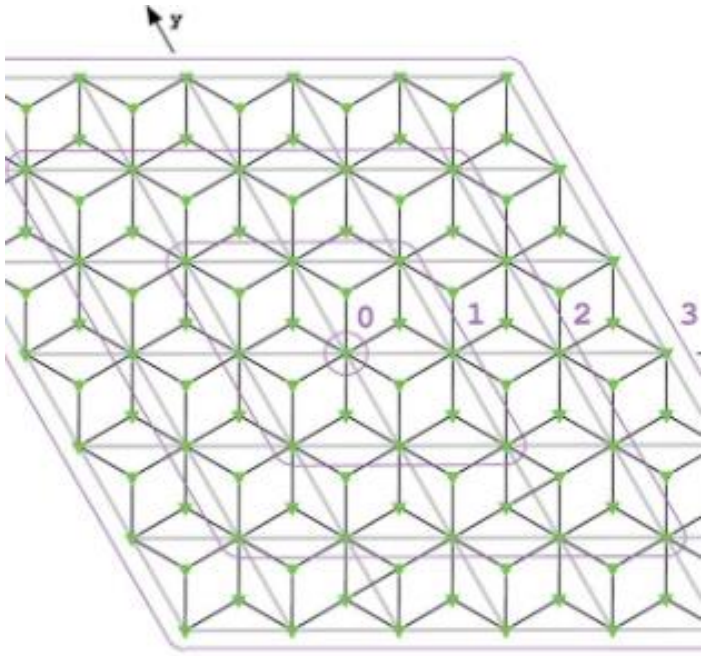
Arithmetic proof of the multiplicity-weighted Euler characteristic for symmetrically arranged space-filling polyhedra.
Acta Cryst. A77, 126-129 (2021)



- We presented a proof of the modified Euler characterstic using only simple arithmetic tools and introducing a notion of **covers** from **algebraic topology.**

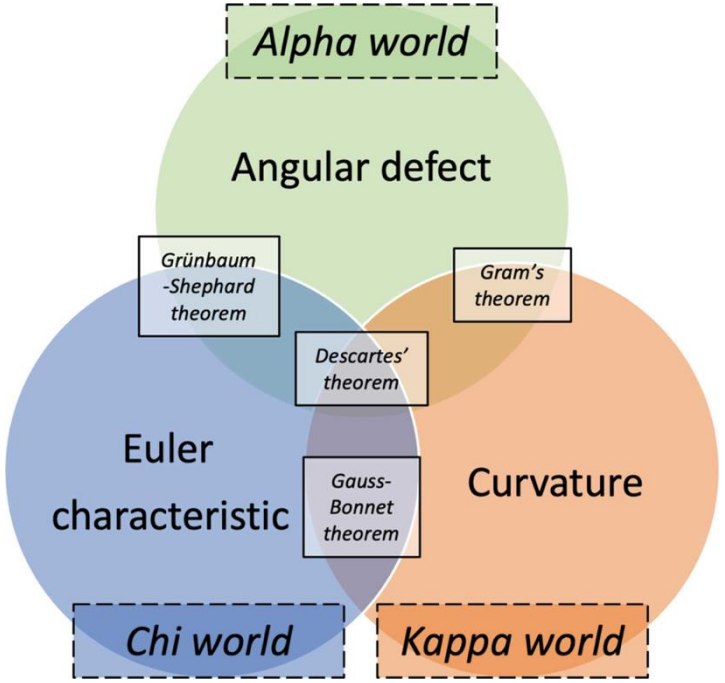
- This opened a possibility for a full proof and turned out to be useful for the study of **growth polynomials** in space tessellations.

A topological proof of the modified Euler characteristic based on the orbifold concept.
Acta Cryst. A77, 317-326 (2021)



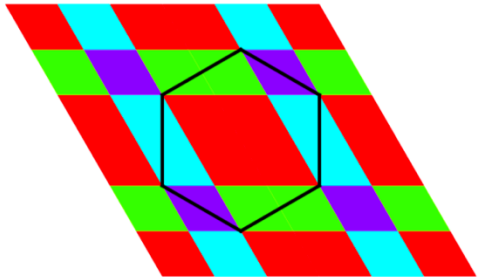
- In this paper we completed the proof of the modified Euler characteristic theorem for **all** crystallographic tessellations in **all** dimensions, connecting it to the work of Coxeter and using sophisticated machinery of **topological orbifolds** (bended spaces with creases and cusps).

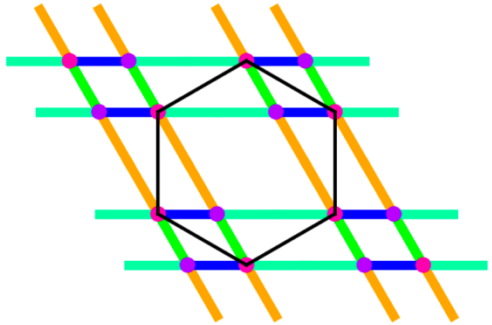
The Euler characteristic as a basis for teaching topology concepts to crystallographers.
J. Appl. Cryst. 55, 154-167 (2022)



- We decided to promote the knowledge and comprehension of the Euler characteristic by introducing this many-faceted notion to a broad community of scientist.
- It turned out that the Euler characteristic is a notion that connects to many branches of mathematics and **has applications** in other sciences.

Growth functions of periodic space tessellations. Acta Cryst A. A81, 64-81 (2025)





- For any periodic tilings of the plane by congruent polygons, growth functions are derived that count the numbers of vertices, edges, and faces as the coverage expands. The functions are computed as polynomial formulas in a Python program and analyzed graphically using orphic diagrams.

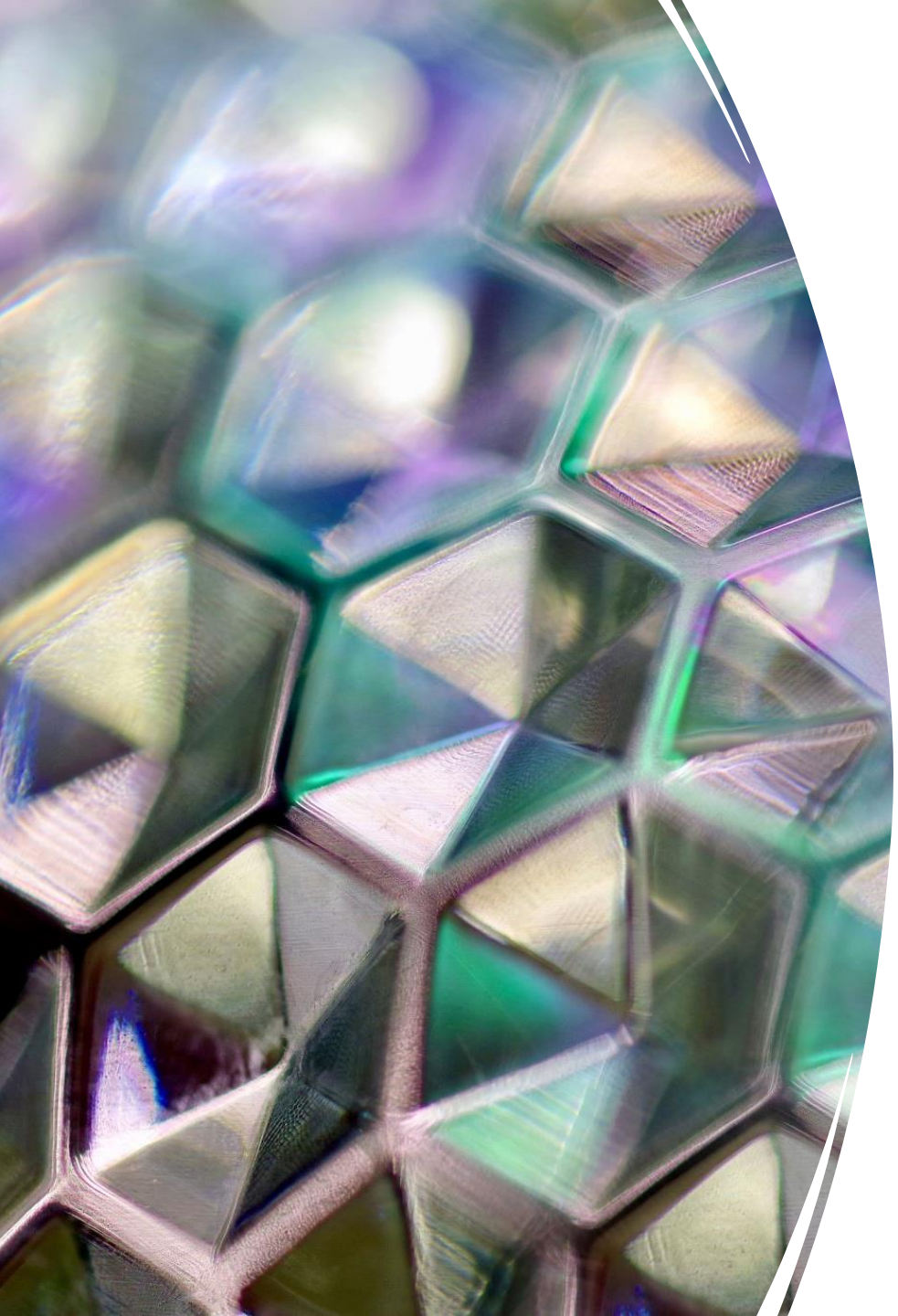
What is a crystal?

- IUCr definition:

*A material is a crystal if it has **essentially** a sharp diffraction pattern.*

This definition encompasses classic periodic structures and quasi-crystals

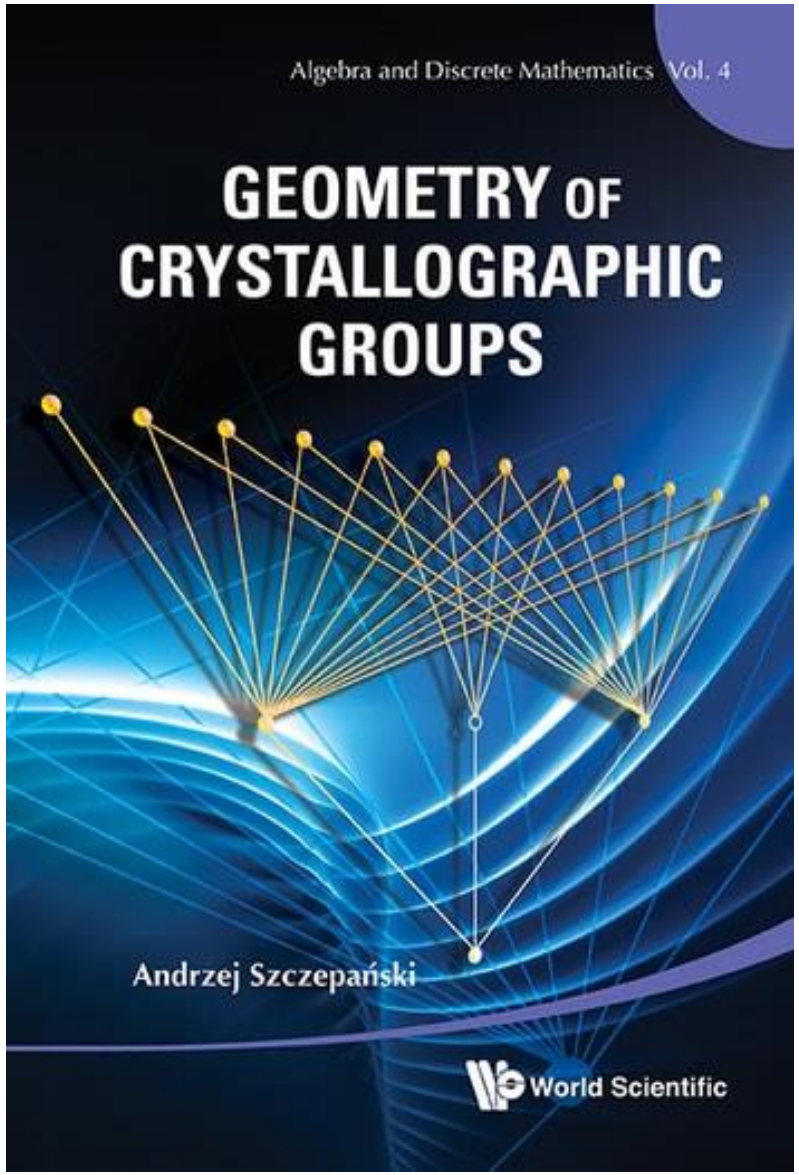
In this talk we discuss periodic structures.

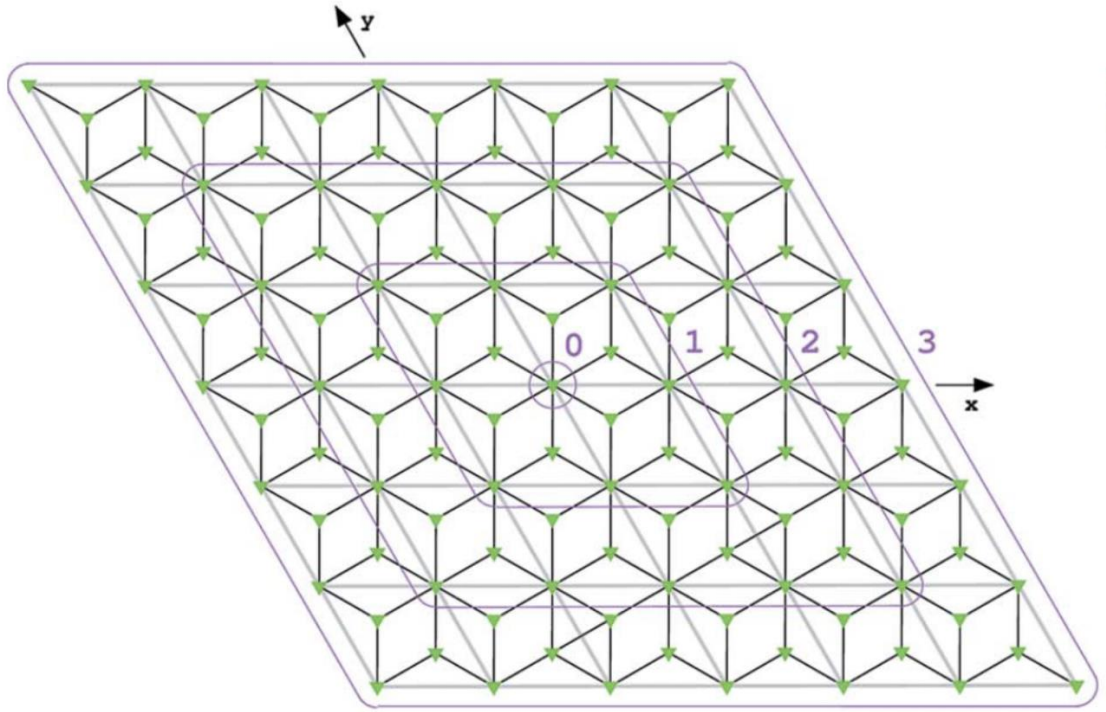


Crystallographic group

- A space group (or Bieberbach group) is a discrete group of isometries of R^n which has a compact fundamental domain
- Bieberbach showed that for general n there is always a finite number of such groups
- For a space group G we have a unique maximal normal abelian subgroup of rank n

$0 \to \mathbb{Z}^n \to G \to P \to 1$, where $P \leq GL_n(\mathbb{Z})$

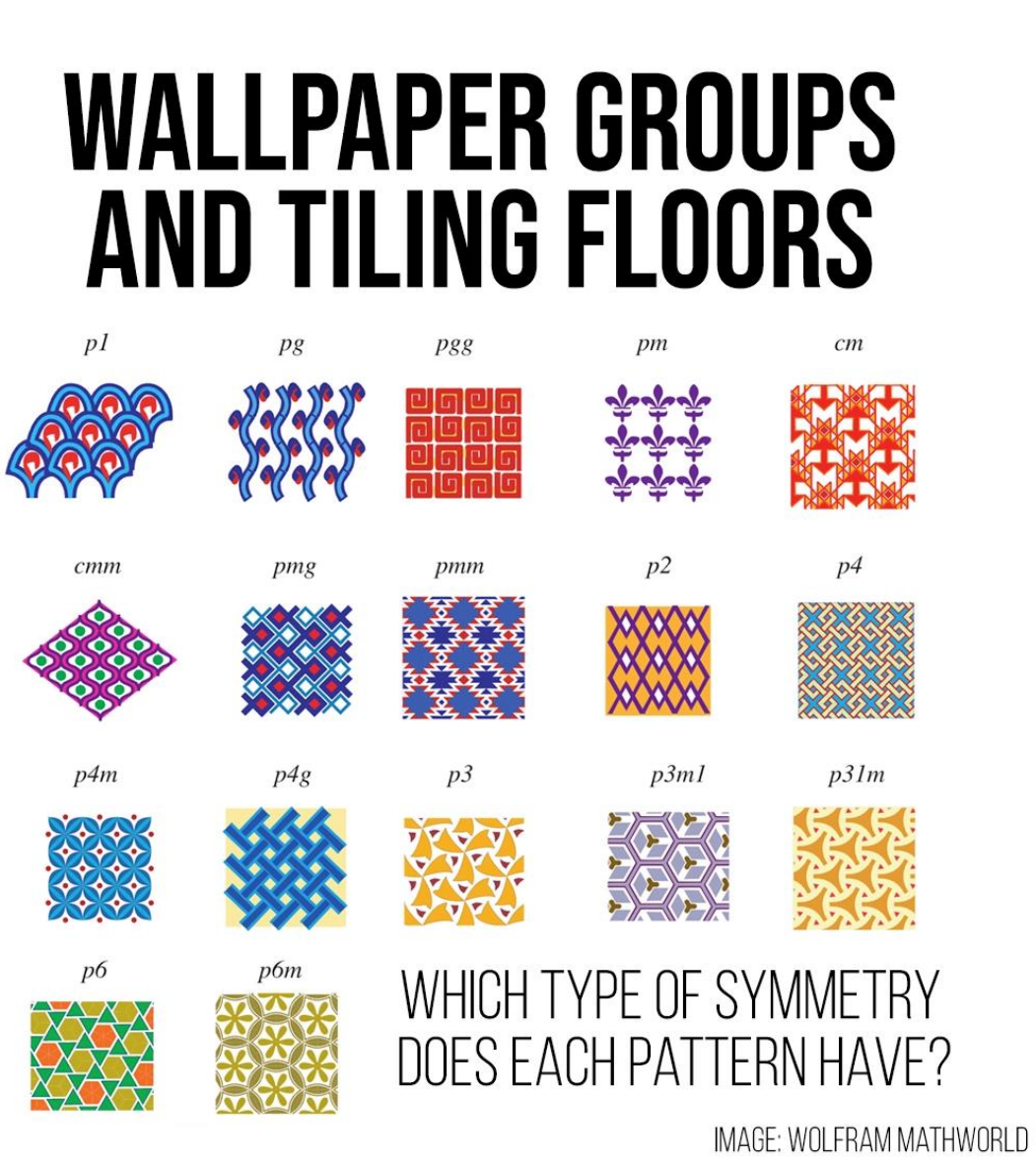

Algebra and Discrete Mathematics Vol. 4
GEOMETRY OF CRYSTALLOGRAPHIC GROUPS
Andrzej Szczepański
World Scientific



p3 wallpaper group (three centers of symmetry)

Wallpaper groups

- In dimension 2 we have 17 isomorphism classes of space groups
- Each group can be associated with infinitely many different tessellations
- Each point group symmetry is of order 1,2,3, 4 or 6

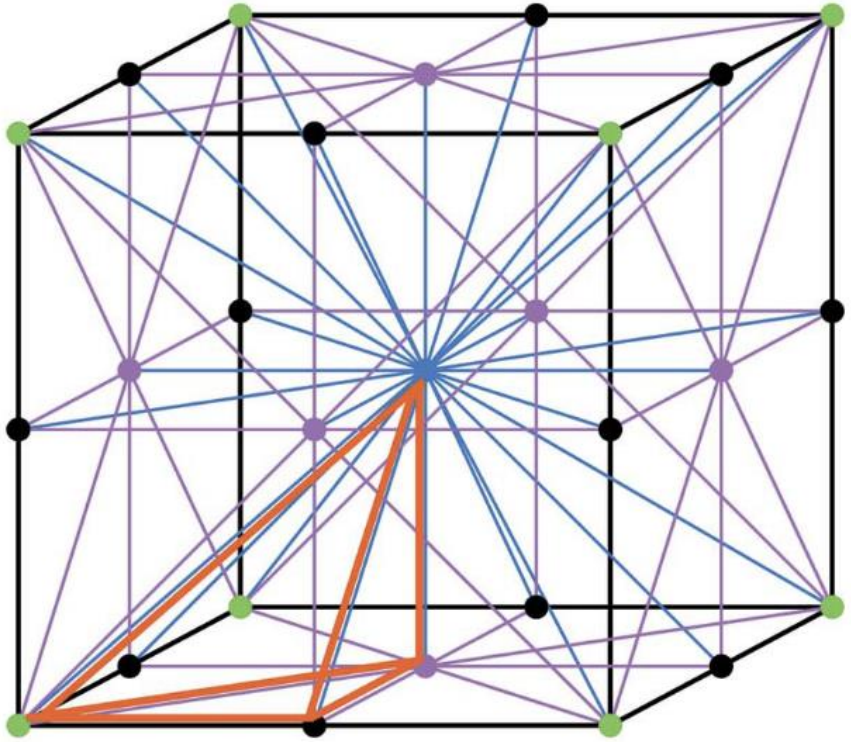


Symmetry group identification

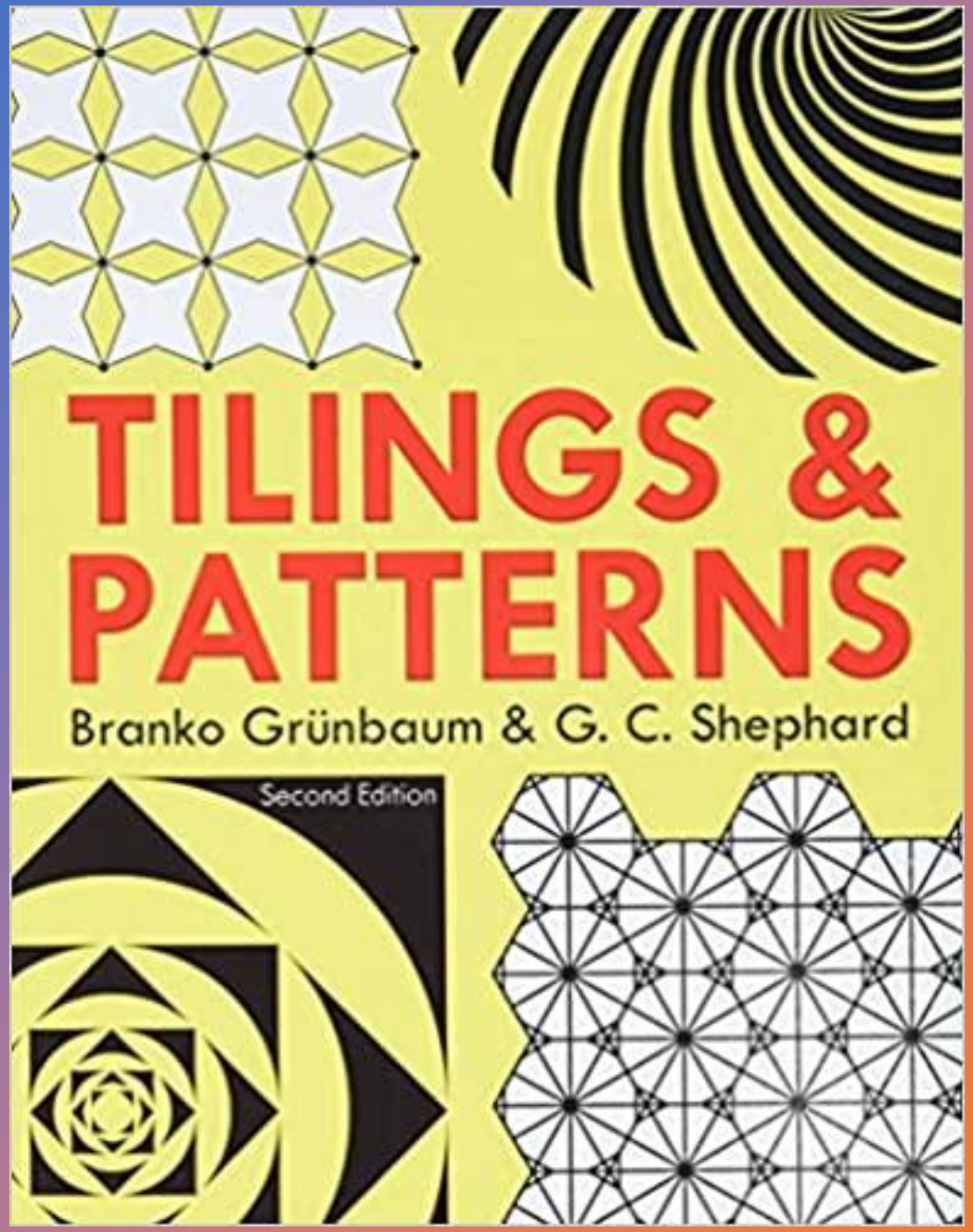
- Each periodic tiling has a unique symmetry group
- There are 17 such groups in 2D
- One can divide group symmetries into simple categories (has reflection?/ point group symmetry order = 1,2,3,4 lub 6)

Space 3D groups

- In 3D we have 230 isomorphism classes of crystallographic groups
- These are symmetries of the 3D crystal structures
- Still no element of order 5 *(elements of order 5 are present in quasicrystals)*
- Beyond dimension 3, we have the following number of groups 4894 (dim 4),222097 (dim 5),??? (dim 6)



$Pm\bar{3}m$ space group



Tessellations

- In this talk we consider tessellations of the Euclidean space which are **normal** in the sense of Grunbaum and Shephard:

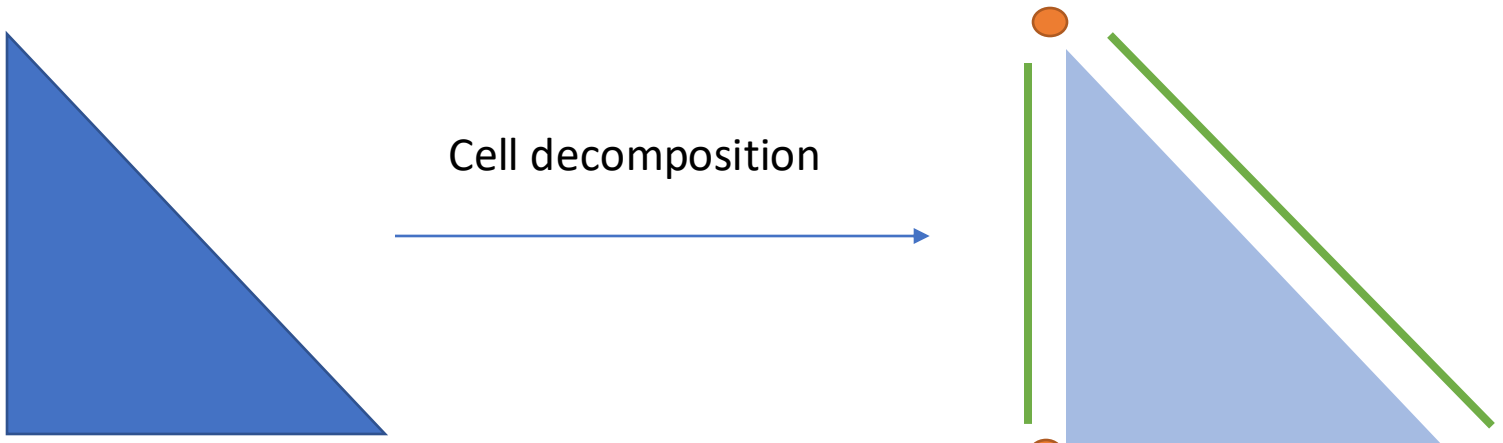
- **1. Every tile is a topological ball**
- **2. The intersection of every two tiles is connected**
- **3. The tiles of the tessellation are uniformly bounded.**

Tessellations as CW-complexes

- Tessellation in this talk is considered as a topological object, i.e. a CW-complex. In particular, this means that we can study its growth properties from the point of view of the combinatorics built into connections between k-dimensional cells of such a complex.
- The sets of k - dimensional cells will be denoted C_k. In particular, for a tessellation in 2D (a tiling) we write $\mathrm{V} = C_0, \mathrm{E} = C_1, \mathrm{F} = C_2$.
- A tessellation is an inductive limit of growing finite tessellations

$$T_0 \subset T_1 \subset T_2 \subset \cdots$$

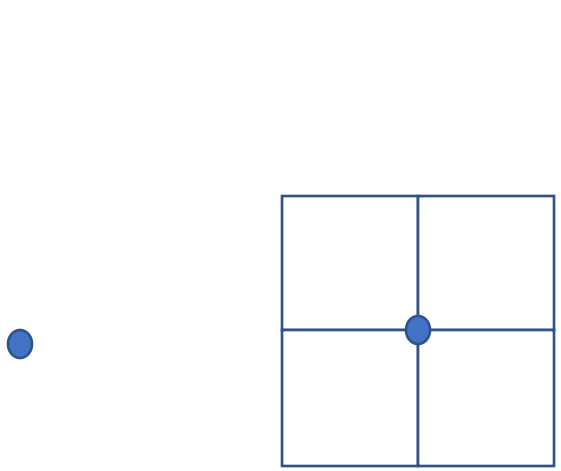
CW complex



Topological space

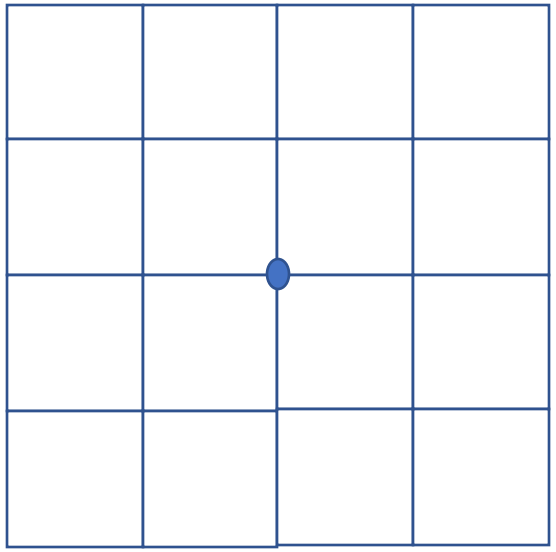
CW complex

Growing tessellation



T_0

T_1



T_2

…

Goal

Our goal is to build numerical invariants of tessellations which can characterize them in various ways (topological, rigid, etc.)

Our starting point was the observation that each regular tessellation (crystallographic) has a unique weighted Euler characteristic

The inputs (over different dimensions) of this modified Euler characteristic can be interpreted as certain coefficients of the growth functions for the expanding tessellation

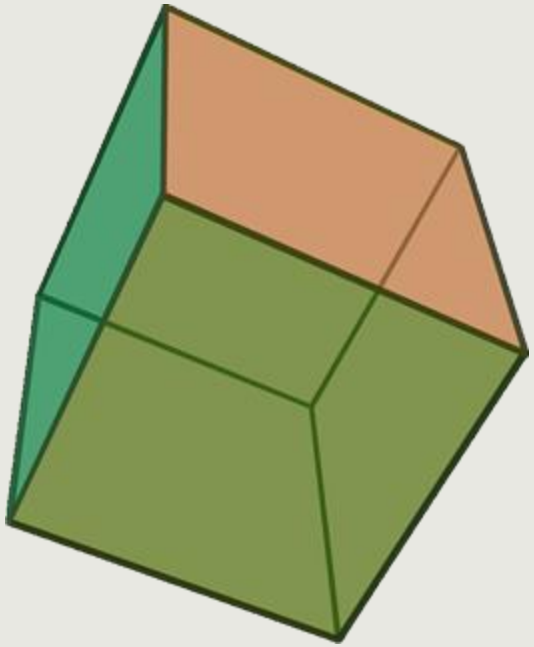
Euler characteristic

- Euler characteristic for polytopes P is the sum $\chi(P) = \sum_i (-1)^i f_i$ of the number of i-dimensional faces.
- For Infinite tessellations this is not **enough** so we need a modified version of this sum

$$\chi_m = \sum_i \sum_j \frac{1}{m_{ij}}$$

where the weight m_{ij} of each j-th i-dimensional cell is computed from the symmetry invariance

for the cube it obviously holds:
8 – 12 + 6 = 2



$$V - E + F = 2$$

The famous Euler's polyhedron formula

relates the number of vertices (V), edges (E) and faces (F)

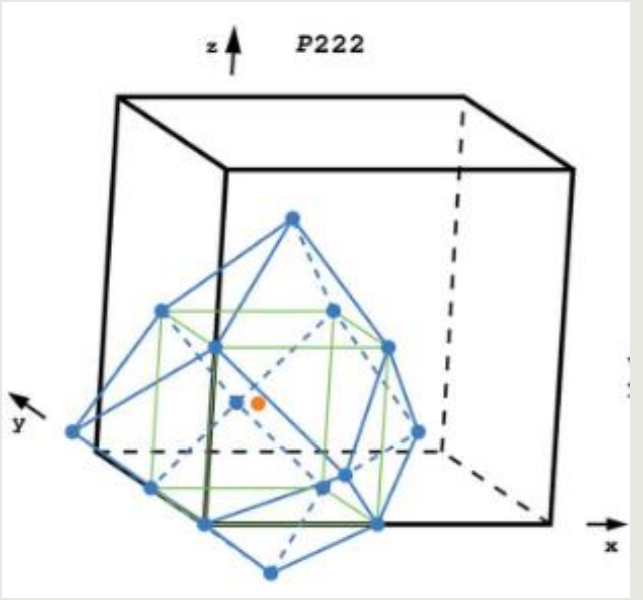
of any polyhedron

Modified Euler characteristic

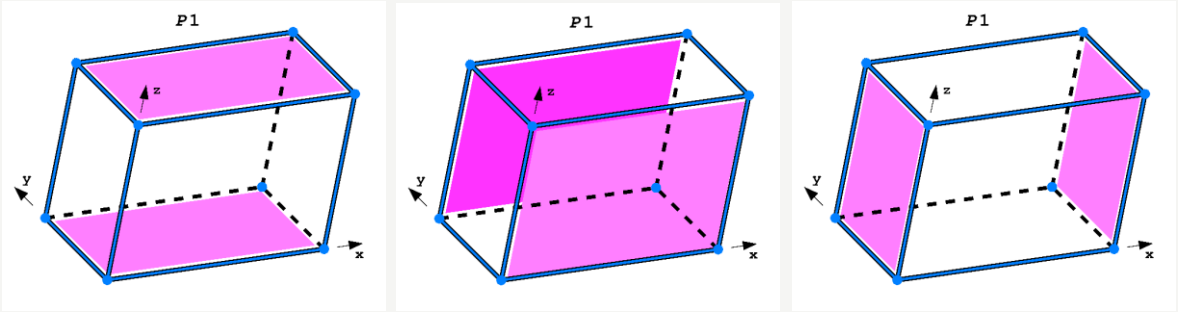
For incomplete polyhedra that are part of an infinite space-filling pattern (tessellation), such as the crystallographic unit cells, asymmetric units, or Dirichlet domains, this formula takes a different, modified form

$$V_m - E_m + F_m = 1$$

This conjecture was published without proof
but with exhaustive examples
by Dauter & Jaskolski (2019) *Acta Cryst.* A**76**, 580-583.



For example, in space group *P*1



- The asymmetric unit has only 3 independent **faces**, $F_m = 3$,

because they are equivalent in parallel pairs.

- Likewise there are only $E_m = 3$ independent **edges** (there is equivalence in all parallel sets);
- And only one **vertex** is independent ($V_m = 1$); the remaining seven are related by **lattice translations**.

Thus: $1 - 3 + 3 = 1$

Orbifolds

- A quotient space $O = \mathbb{R}^n/G$ has a natural structure of an orbifold (Satake, Thurston). It is a Hausdorff space where $O \setminus \Sigma$ is a manifold and every point in the **singular set** Σ has fractional neighborhood.

- Since the crystallographic group G has finite index full rank abelian subgroup, we have a finite (orbifold) cover $\mathbb{T} \to O$ by a torus of dimension n

Orbifold p3

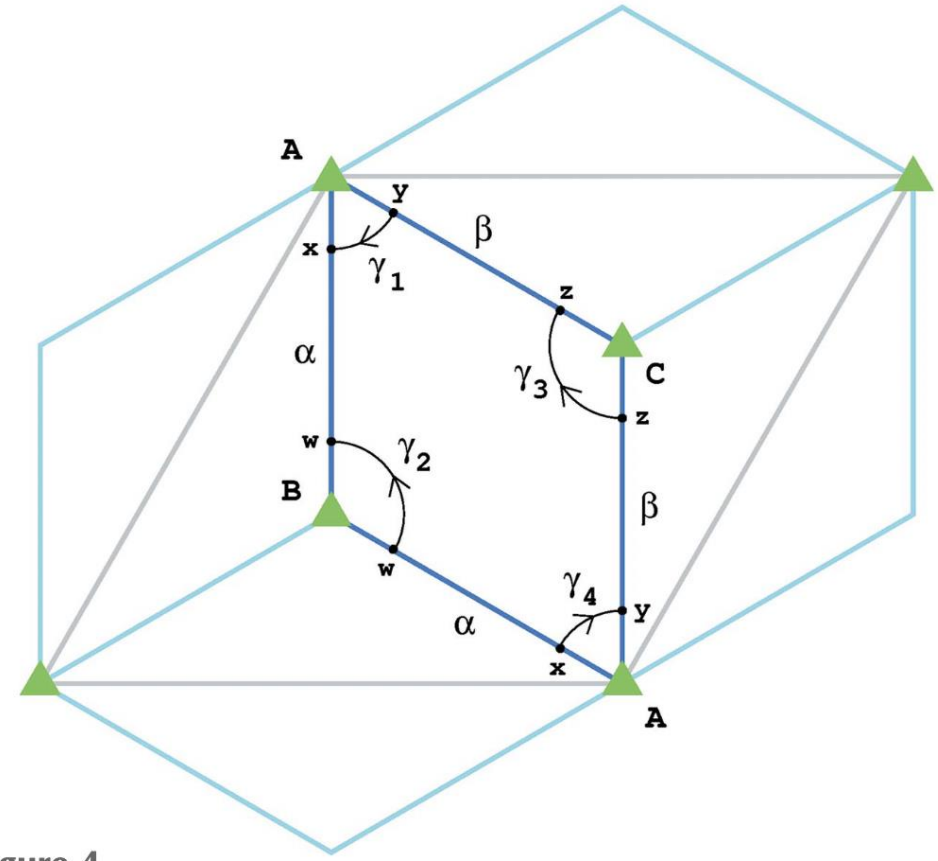


Figure 4
The unit cell (gray edges) and the ASU (blue edges) with four adjacent copies of the ASU (light blue) of the wallpaper group $p3$. The green triangles indicate points with rotational threefold symmetry. The arcs indicate the closed paths around singular points of the orbifold $\mathcal{O}_{p3}$ and the labels α, β indicate identified edges. See text for further details.

Orbifold Pcc2

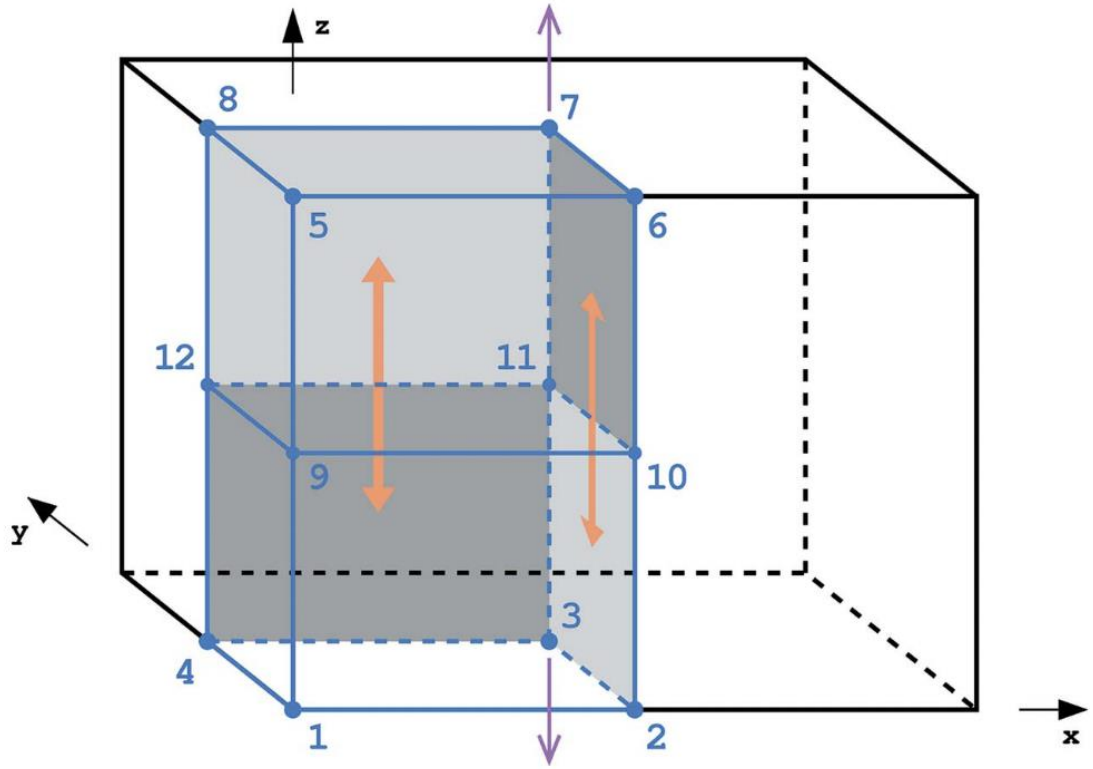


Figure 5
The unit cell (black edges) and ASU (blue edges) of the orthorhombic space group *Pcc*2. Only some relevant symmetry elements are marked, the twofold axis in purple and the glide *c*-planes indicated by orange arrows. Additional parallel twofold axes pass through all corners and half-edges of the cell, and additional glide planes lie at all vertical faces of the unit cell.

Orbifold weights

- A CW structure on $\mathbb{R}^n$ which is **compatible** with the action of the space group G induces a **CW structure** on the orbifold $O = \mathbb{R}^n/G$
- Each cell σ has a weight which is $1/|\Gamma(\sigma)|$ where $\Gamma(\sigma)$ is a finite stabilizer subgroup of σ in G
- Orbifold Euler characteristic is

$$\chi(O) = \sum_{\sigma} (-1)^{dim\sigma} \frac{1}{|\Gamma(\sigma)|}$$

Modified Euler characteristic

- Key fact: for a finite orbifold cover $O_1 \to O_2$ we have $\chi(O_1) = d\chi(O_2)$ where d is the degree of the cover

Theorem

For every crystallographic group G, the orbifold

$$\mathbb{R}^n/G$$

has orbifold Euler characteristic 0.

Coxeter's growth functions

- The orbifold weights vector:

$$u(O) = \left(\sum_{dim\sigma=0} \frac{1}{|\Gamma(\sigma)|}, \cdots, \sum_{dim\sigma=n} \frac{1}{|\Gamma(\sigma)|} \right)$$

has a natural interpretation in terms of the certain growth functions of the tessellation associated with O

- For each dimension j we fix a starting vertex and count as $N_j(R)$ the number of j-dim cells contained in the ball of radius R.

Functorialization of orbifold weights

- It was shown by Coxeter (on a number of examples that) the limits

$$v_j = \lim_{j\to\infty} N_j(R)/R^n$$

exist and satisfy $\sum_j (-1)^j v_j = 0$

Theorem

There exists a constant C ($= |pt(G)| \cdot vol(unit\ ball)/vol(unit\ cell)$) such that

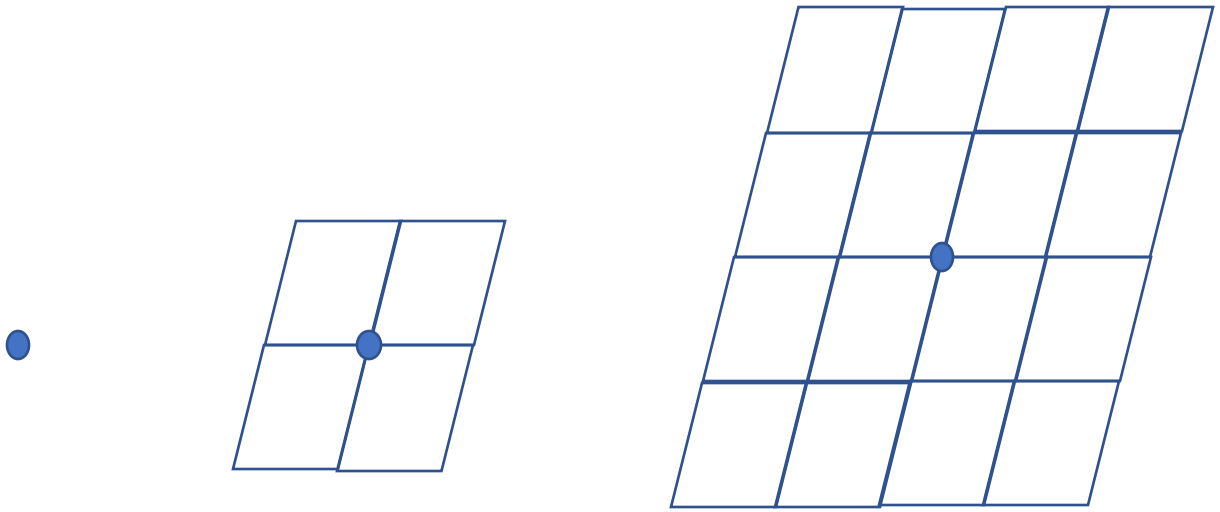
$$u(O) = C\ (v_0, \dots, v_n)$$

Topological growth functions

- When we choose a natural graph metric (distance measured by path steps) we have growth functions $f_i(n)$ which count the number of i-dim cells within n-steps from the starting vertex

- Each function $f_i(n)$ is a degree i polynomial in variable n with **integer** coefficients. The vector of leading terms of these functions is proportional to $u(O)$!

Growth polynomials for P1



T_0 T_1 T_2

$$f_0(n) = 1 \cdot (2n)^2 + 2(2n) + 1$$

$$f_1(n) = 2 \cdot (2n)^2 + 2(2n)$$

$$f_2(n) = 1 \cdot (2n)^2$$

Orbifold is a T^2 torus, orbifold numbers are Betti numbers (1,2,1).

Topological growth functions

G	$N_k(n)$	Vector $u(\mathcal{O}_\Gamma)$	Figure
$p3$	$N_0(n) = 12n^2 + 4n + 1$ $N_1(n) = 24n^2$ $N_2(n) = 12n^2 - 4n$	$(3 \cdot 1/3, 2 \cdot 1, 1)$	$3(a)$
$p6$	$N_0(n) = 24n^2 + 8n + 1$ $N_1(n) = 48n^2 + 8n$ $N_2(n) = 24n^2$	$(1/6 + 1/3 + 1/2, 1 + 1, 1)$	$3(b)$
$p6m$	$N_0(n) = 24n^2 + 8n + 1$ $N_1(n) = 72n^2 + 8n$ $N_2(n) = 48n^2$	$(1/12 + 1/6 + 1/4, 3 \cdot 1/2, 1)$	$3(c)$
$P23$	$N_0(n) = 64n^3 + 48n^2 + 12n + 1$ $N_1(n) = 352n^3 + 144n^2 + 12n$ $N_2(n) = 384n^3 + 96n^2$ $N_3(n) = 96n^3$	$(2 \cdot 1/12 + 2 \cdot 1/4, 4 \cdot 1/2 + 2 \cdot 13 + 1, 4 \cdot 1, 1)$	$6(a)$
$Pm\bar{3}m$	$N_0(n) = 64n^3 + 48n^2 + 12n + 1$ $N_1(n) = 448n^3 + 144n^2 + 12n$ $N_2(n) = 768n^3 + 96n^2$ $N_3(n) = 384n^3$	$(2 \cdot 1/48 + 2 \cdot 1/16, 2 \cdot 1/8 + 3 \cdot 1/4 + 1/6, 4 \cdot 1/2, 1)$	$6(b)$

Topological growth functions

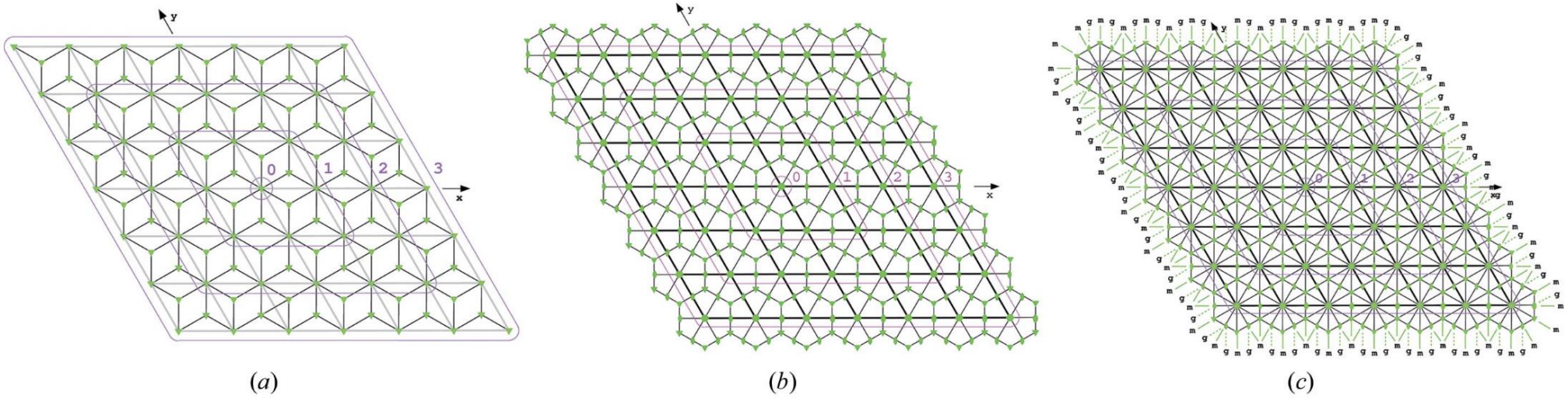
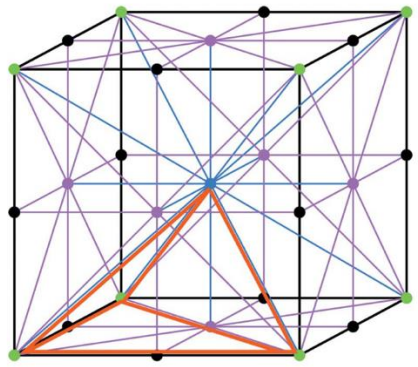
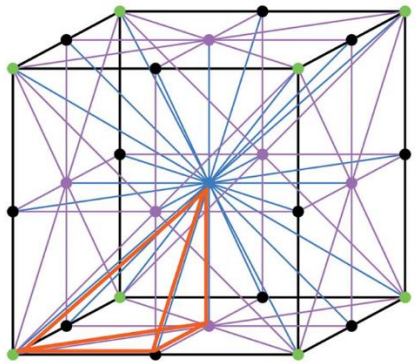


Figure 3
Orbifold ASU tessellation of the groups (*a*) *p*3, (*b*) *p*6 and (*c*) *p6mm*. A purple rhombus of index *i* represents a region which encircles the elements of the tessellation which are subject to a counting function with parameter *i*.

Topological growth functions



(*a*)



(*b*)

Figure 6
Orbifold ASU (bold red lines) of the space groups (*a*) *P*23 and (*b*) $Pm\bar{3}m$.

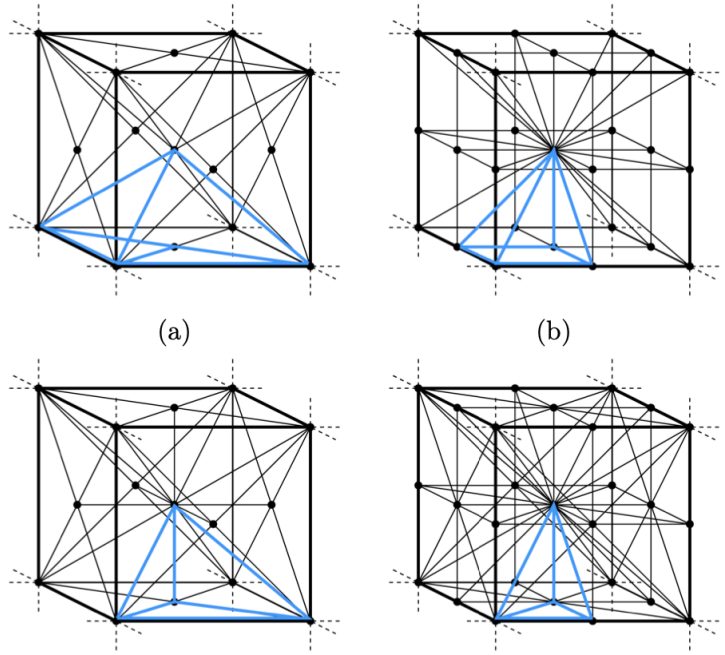


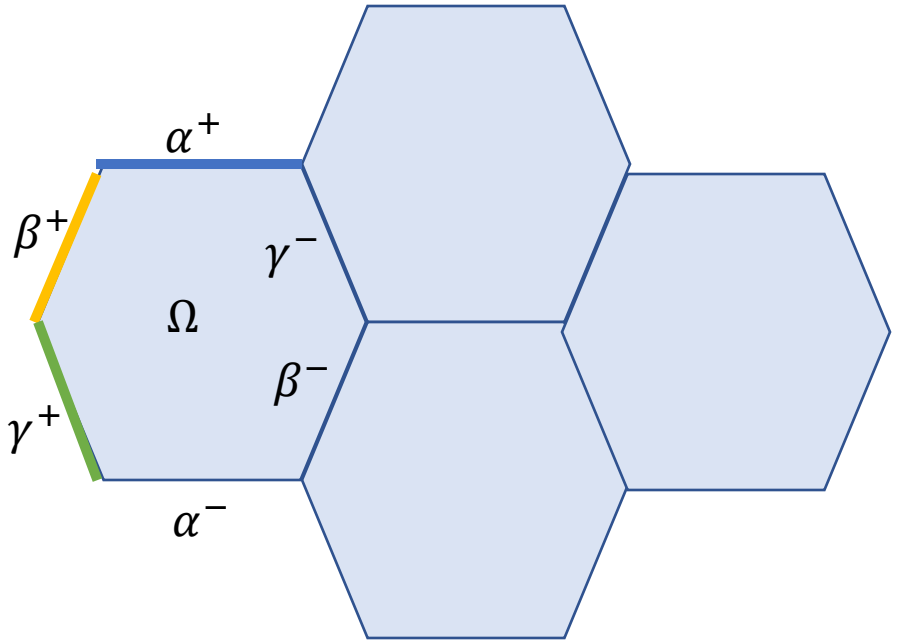
Fig. 11. The unit cells of the primitive cubic symmorphic space groups, divided into individual asymmetric units, with one asymmetric unit highlighted in blue. a) $P23$, b) $Pm\bar{3}$, c) $P432$ and $P\bar{4}3m$, d) $Pm\bar{3}m$.

Table 5. *Crystallographic growth polynomials (of single variable n) of all elements of the unit cells shown in Fig. 11.*

Space group	V	E	F	I
$P23$	$5n^3+6n^2+3n+1$	$23n^3+18n^2+3n$	$30n^3+12n^2$	$12n^3$
$Pm\bar{3}$	$8n^3+12n^2+6n+1$	$44n^3+24n^2+6n$	$60n^3+12n^2$	$24n^3$
$P432$ and $P\bar{4}3m$	$5n^3+6n^2+3n+1$	$29n^3+18n^2+3n$	$48n^3+12n^2$	$24n^3$
$Pm\bar{3}m$	$8n^3+12n^2+6n+1$	$56n^3+36n^2+6n$	$96n^3+24n^2$	$48n^3$

2D crystal types

- In two dimensions we have a more refined prediction of the growth functions which depends on the combinatorial data of the fundamental unit of the tessellation with respect to the translation subgroup



2d crystal types

Proposition 3.5. For a given periodic tessellation $\mathcal{T}$ with domain Ω we have the following growth polynomials $(f_0(n), f_1(n), f_2(n))$ expressed in the graph radius n.

Case (I) polynomials

$$f_0(n) = (|\Omega_0| - (1 + |\alpha^+| + |\beta^+|)) \cdot (2n)^2 + (|\alpha^+| + |\beta^+|) \cdot (2n) + 1,$$
$$f_1(n) = (|\Omega_1| - (|\alpha^+| + |\beta^+|)) \cdot (2n)^2 + (|\alpha^+| + |\beta^+|) \cdot (2n),$$
$$f_2(n) = |\Omega_2| \cdot (2n)^2,$$

Case (II) polynomials

$$f_0(n) = (|\Omega_0| - (1 + |\alpha^+| + |\beta^+| + |\gamma^+|)) \cdot (2n)^2 + (|\alpha^+| + |\beta^+| + 2|\gamma^+|) \cdot (2n) + 1 - |\gamma^+|,$$
$$f_1(n) = (|\Omega_1| - (|\alpha^+| + |\beta^+| + |\gamma^+|)) \cdot (2n)^2 + (|\alpha^+| + |\beta^+| + 2|\gamma^+|) \cdot (2n) - |\gamma^+|,$$
$$f_2(n) = |\Omega_2| \cdot (2n)^2,$$

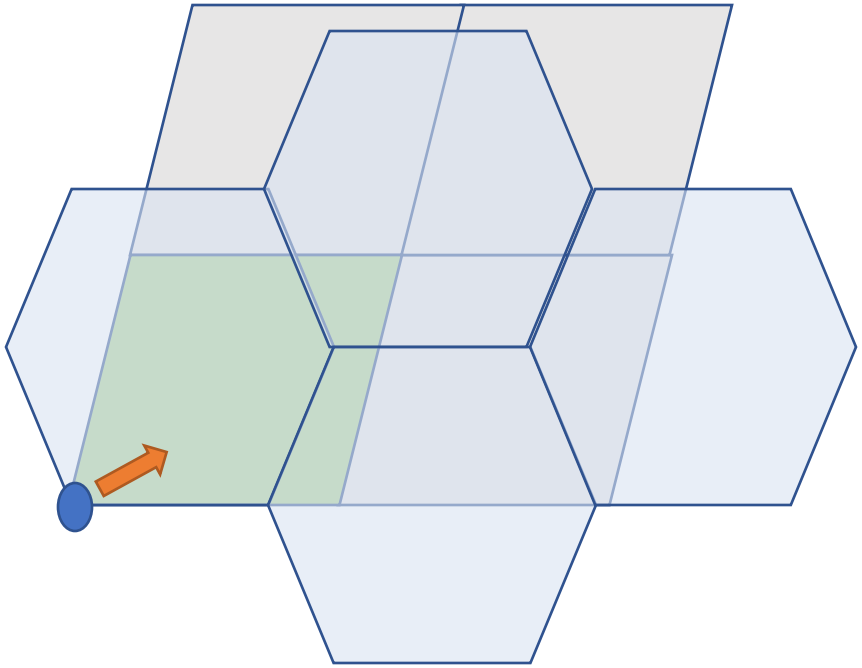
Application of topological growth functions

- Topological growth functions are insensitive to the topological deformation of the tessellation, i.e. they encode some aspects of the tessellation CW-compex connectivity
- E.g. one can use it to distinguish a topological type of the tessellation once given partial or corrupted data

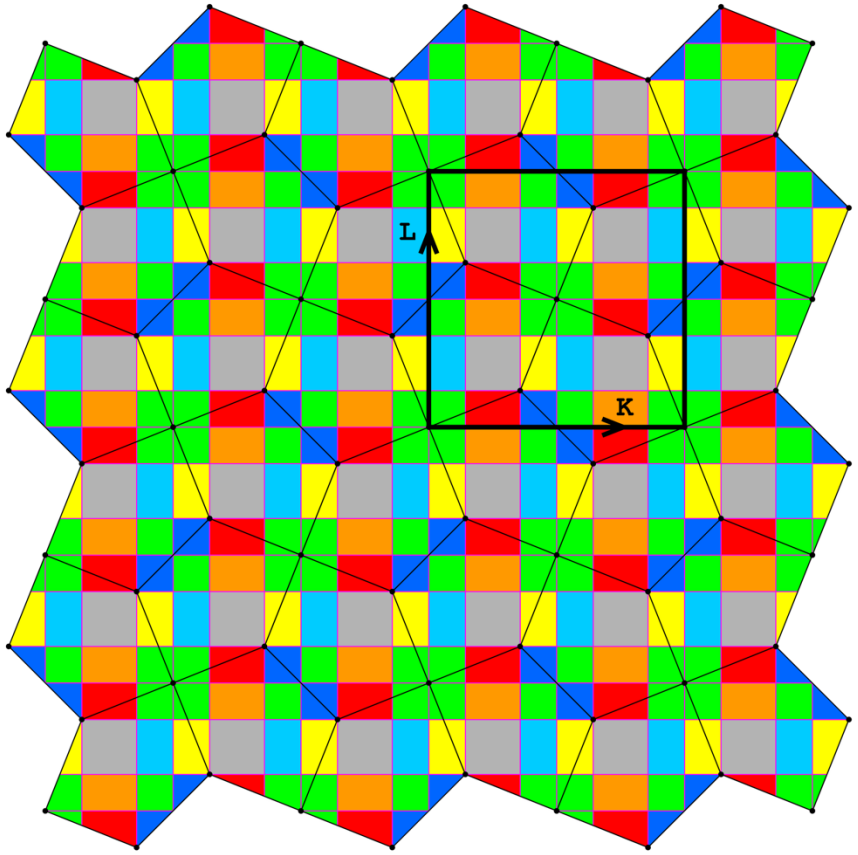
p\n	1	4	9	16
0.0100000000000000	[884] 0 || [444] 953 || Other 47	[884] 0 || [444] 998 || Other 2	[884] 0 || [444] 1000 || Other 0	[884] 0 || [444] 1000 || Other 0
0.100000000000000	[884] 0 || [444] 671 || Other 329	[884] 17 || [444] 787 || Other 196	[884] 0 || [444] 985 || Other 15	[884] 0 || [444] 998 || Other 2
0.200000000000000	[884] 2 || [444] 429 || Other 569	[884] 95 || [444] 581 || Other 324	[884] 11 || [444] 924 || Other 65	[884] 4 || [444] 984 || Other 12
0.500000000000000	[884] 63 || [444] 66 || Other 871	[884] 396 || [444] 124 || Other 480	[884] 406 || [444] 433 || Other 161	[884] 567 || [444] 386 || Other 47
0.800000000000000	[884] 400 || [444] 1 || Other 599	[884] 672 || [444] 1 || Other 327	[884] 929 || [444] 11 || Other 60	[884] 978 || [444] 2 || Other 20
0.900000000000000	[884] 668 || [444] 0 || Other 332	[884] 863 || [444] 0 || Other 137	[884] 989 || [444] 1 || Other 10	[884] 999 || [444] 0 || Other 1
0.990000000000000	[884] 969 || [444] 0 || Other 31	[884] 999 || [444] 0 || Other 1	[884] 1000 || [444] 0 || Other 0	[884] 1000 || [444] 0 || Other 0

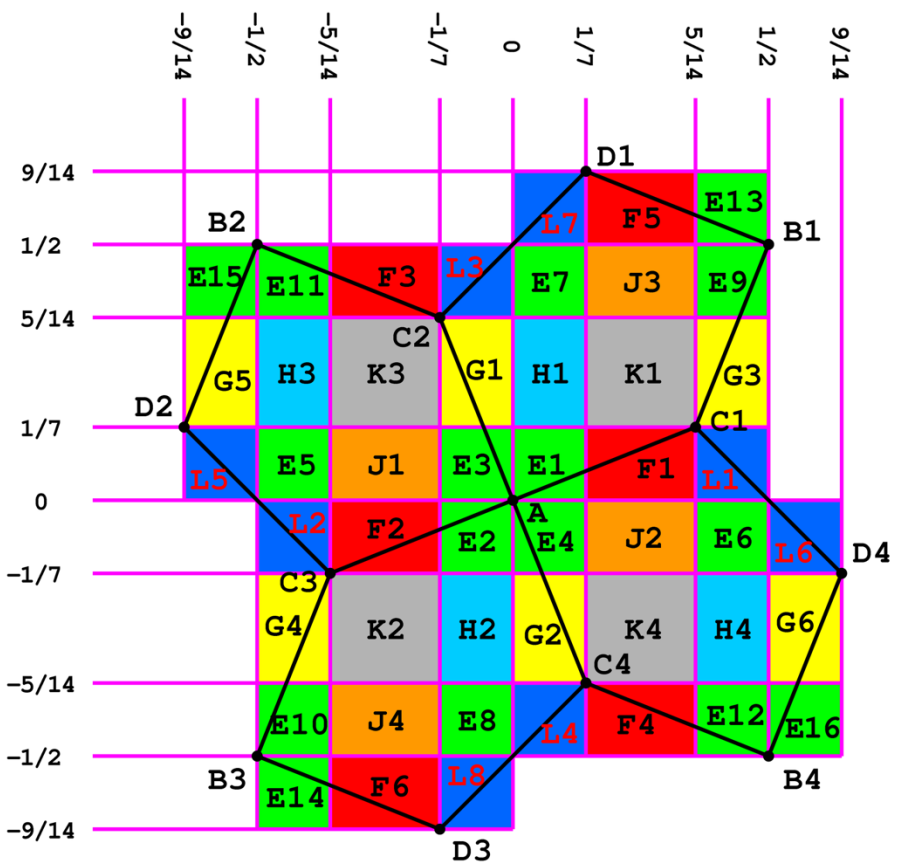
Crystallographic growth functions

- Studying various metrics leads to different growth functions (Coxeter's ball growth, topological growth)
- We investigate **crystallographic growth functions** where the stratification $\{T_n\}$ of the tessellation T is given by the natural unit cell frames

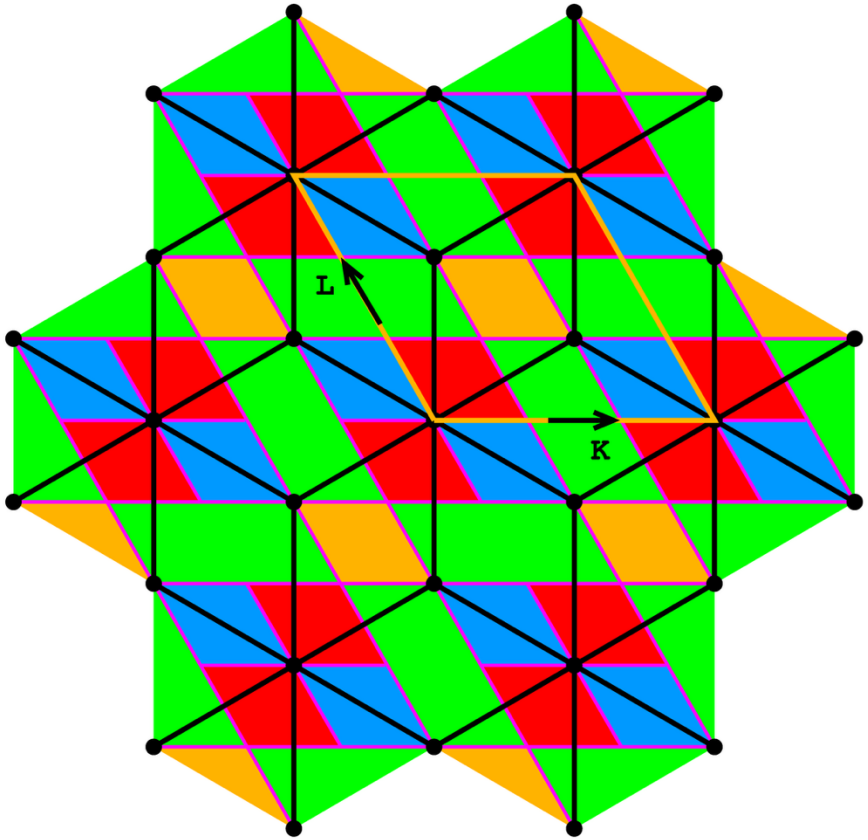


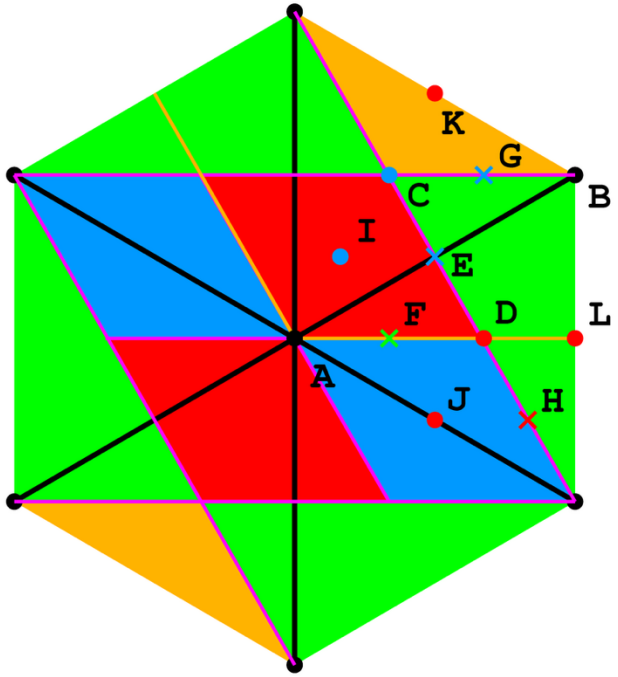
43433 (vertex degree) tessellation



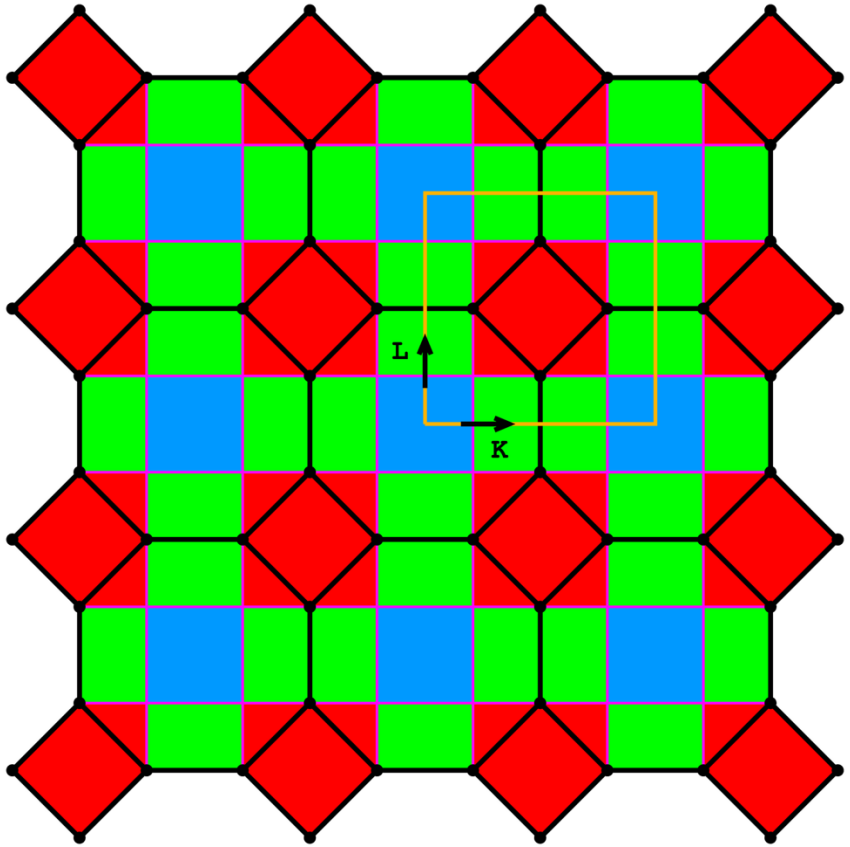


6363 tessellation





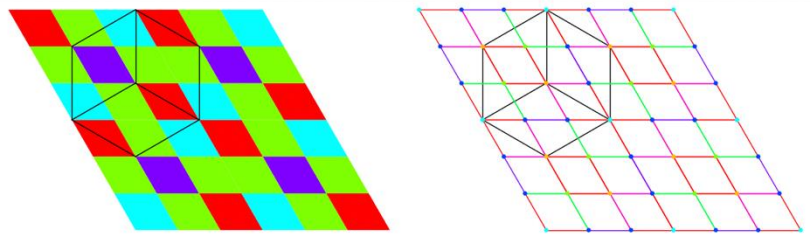
884 dual tessellation



Python and Julia package demo

```
In [7]: import crystgrowthpoly as cryst
        tes = cryst.read_tessellation_from_file("./tesselations/6363.txt",  crystalographic_coordinates=True,cartesian_vec
        tes.plot_domains(full_plot=True)
```

Out[7]:



```
**************************
For x_0 in
Parallelogram  ((2/3, 2/3), (1, 2/3), (1, 1), (2/3, 1))
Parallelogram  ((0, 0), (1/3, 0), (1/3, 1/3), (0, 1/3))
```

$f_0(n)=3n^2$

$f_1(n)=6n^2-6n+2$

$f_2(n)=3n^2-6n+3$

```
**************************
**************************
For x_0 in
Parallelogram  ((1/3, 1/3), (2/3, 1/3), (2/3, 2/3), (1/3, 2/3))
```

$f_0(n)=3n^2$

$f_1(n)=6n^2-4n$

$f_2(n)=3n^2-4n+1$

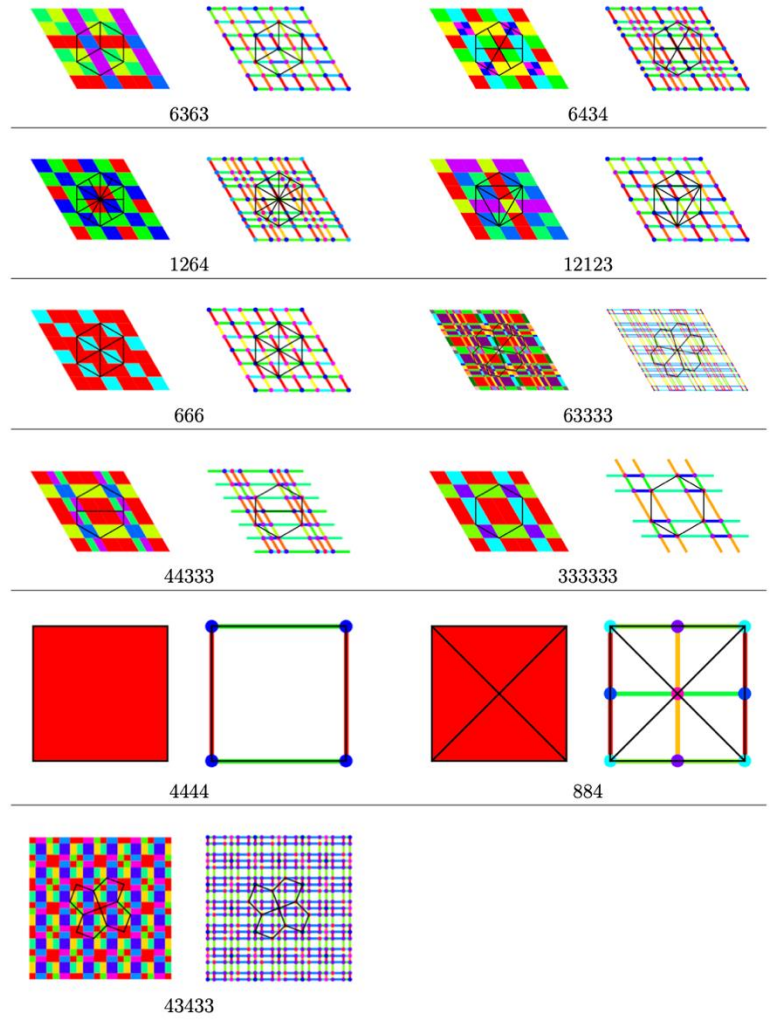
```
**************************
**************************
For x_0 in
Line  ((1/3, 1/3), (1/3, 2/3))
Line  ((2/3, 0), (1, 0))
Line  ((0, 0), (0, 1/3))
Line  ((1, 0), (1, 1/3))
Line  ((1/3, 1/3), (2/3, 1/3))
Line  ((2/3, 1/3), (2/3, 2/3))
Line  ((1/3, 2/3), (2/3, 2/3))
Line  ((1/3, 1/3), (1/3, 2/3))
Line  ((1/3, 1/3), (2/3, 1/3))
Line  ((0, 1), (1/3, 1))
Line  ((0, 2/3), (0, 1))
Line  ((1/3, 2/3), (2/3, 2/3))
Line  ((2/3, 1/3), (2/3, 2/3))
Line  ((1, 2/3), (1, 1))
Line  ((2/3, 1), (1, 1))
Line  ((0, 0), (1/3, 0))
```

$f_0(n)=3n^2+n$

$f_1(n)=6n^2-3n$

$f_2(n)=3n^2-4n+1$

```
**************************
**************************
For x_0 in
```



Malinowski, J., (2022). Orphic diagrams: Python package for computing growth functions of planar tessellations; DOI:10.5281/zenodo.7275212.

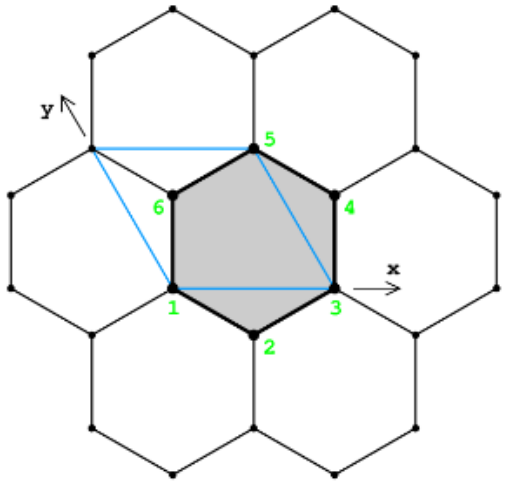
Malinowski, J. (2023). Orphic diagrams: Julia package, Cocalc Eucrypol

Computational setup

- We will consider a periodic tessellation, otherwise known as tiling.
- Tiles are set up with a list of vertices, edges and faces, and two translation vectors.
- A tile must cover the whole plain

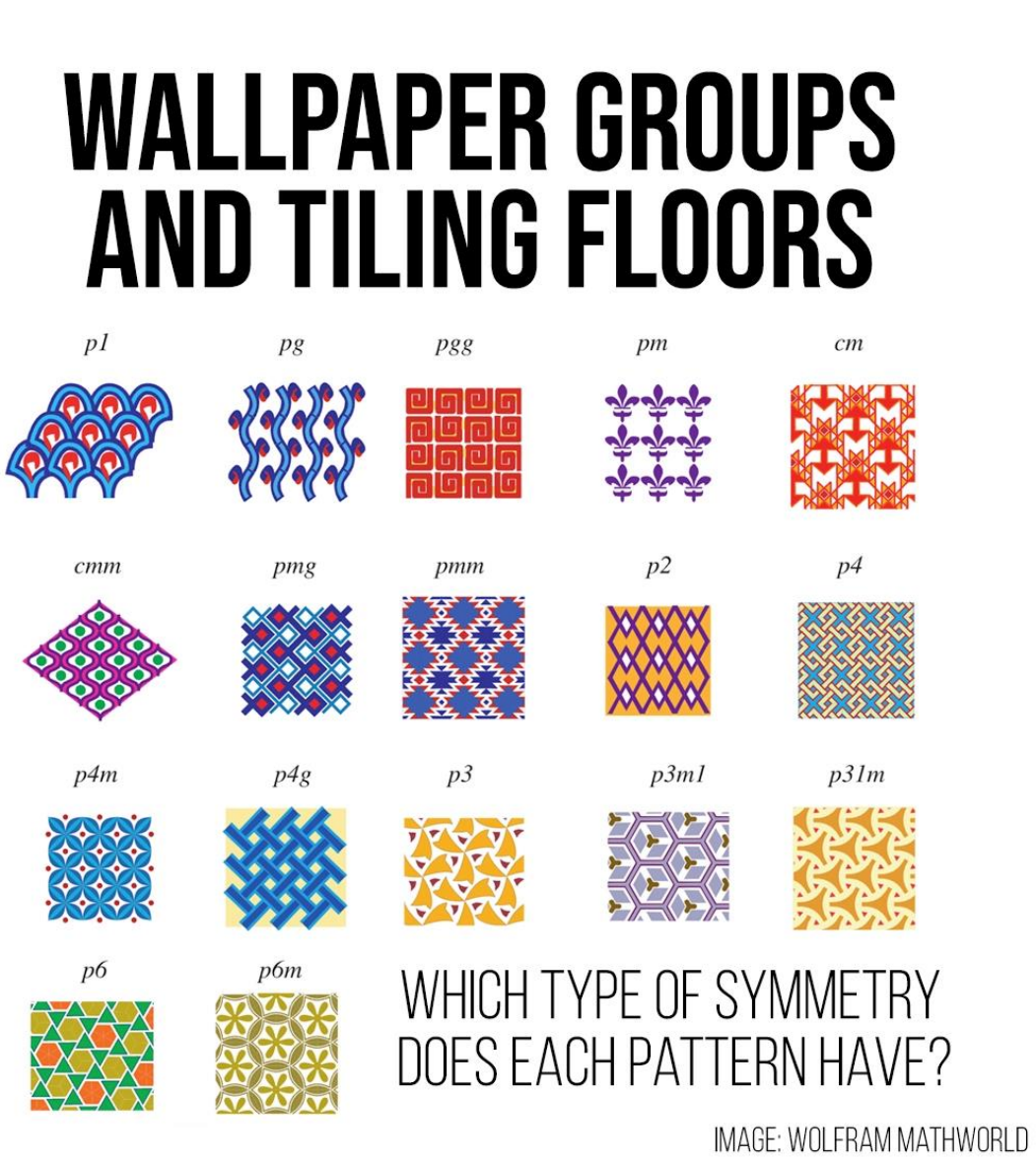
```
6 6 1
  0      0
  1/3   -1/3
  1      0
  4/3    2/3
  1      1
  1/3    2/3
1 2
2 3
3 4
4 5
5 6
6 1
1 2 3 4 5 6
1 0
-1/2 sqrt(3)/2
```

(a)



(b)

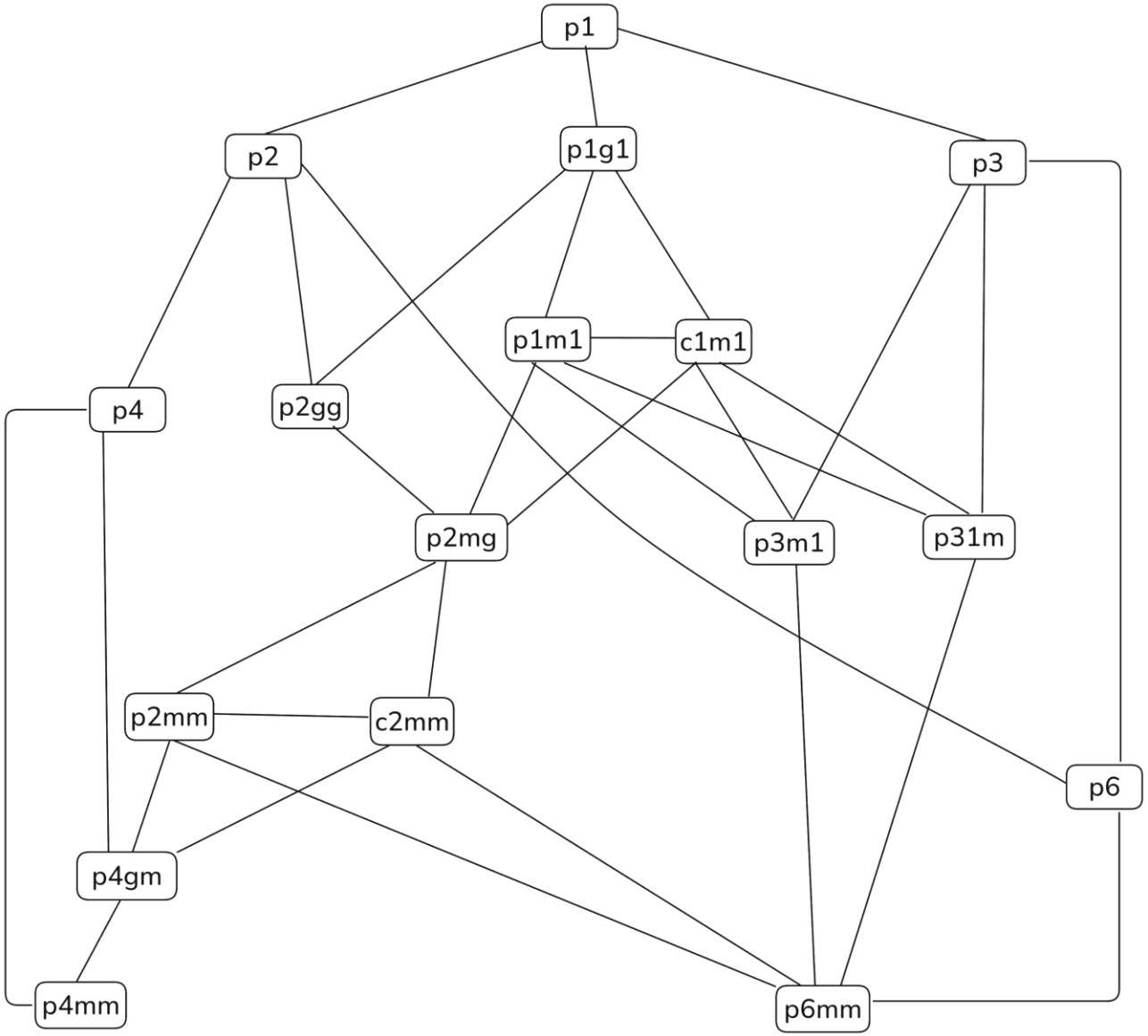
Fig. 11. Sample input (a) encoding the 333333 tiling (b). The line 6 6 1 (red) gives V E F, where V is the number of vertices, E is the number of edges, and F is the number of faces. The next 6 (V) lines (green) describe the crystallographic coordinates of the vertices. The next 6 (E) (black) lines describe the connectivity of the vertices (i.e., edges). Finally, the next 1 (F) (red) line(s) describe the faces. The last two (blue) lines specify the translational lattice.



Symmetry group identification

- Each periodic tiling has a unique symmetry group
- There are 17 such groups in 2D
- One can divide group symmetries into simple categories (has reflection?/ point group symmetry order = 1,2,3,4 lub 6)

Group relations



Group symmetry identification

- Identification of the group is based on the type of geometry. This can be summarized by a simple table.
- In teaching these types of symmetry, you can focus only on single properties

Guide to recognizing wallpaper groups [edit]

To work out which wallpaper group corresponds to a given design, one may use the following table.[4]

<table>
<tr><td rowspan="2">Size of smallest rotation</td><td colspan="5">Has reflection?</td></tr>
<tr><td colspan="3">Yes</td><td colspan="2">No</td></tr>
<tr><td>360° / 6</td><td colspan="3">p6m (*632)</td><td colspan="2">p6 (632)</td></tr>
<tr><td rowspan="2">360° / 4</td><td colspan="3">Has mirrors at 45°?</td><td colspan="2" rowspan="2">p4 (442)</td></tr>
<tr><td colspan="2">Yes: p4m (*442)</td><td>No: p4g (4*2)</td></tr>
<tr><td rowspan="2">360° / 3</td><td colspan="3">Has rot. centre off mirrors?</td><td colspan="2" rowspan="2">p3 (333)</td></tr>
<tr><td colspan="2">Yes: p31m (3*3)</td><td>No: p3m1 (*333)</td></tr>
<tr><td rowspan="4">360° / 2</td><td colspan="3">Has perpendicular reflections?</td><td colspan="2" rowspan="2">Has glide reflection?</td></tr>
<tr><td colspan="2">Yes</td><td>No</td></tr>
<tr><td colspan="2">Has rot. centre off mirrors?</td><td rowspan="2">pmg (22*)</td><td rowspan="2">Yes: pgg (22×)</td><td rowspan="2">No: p2 (2222)</td></tr>
<tr><td>Yes: cmm (2*22)</td><td>No: pmm (*2222)</td></tr>
<tr><td rowspan="2">none</td><td colspan="3">Has glide axis off mirrors?</td><td colspan="2">Has glide reflection?</td></tr>
<tr><td colspan="2">Yes: cm (*×)</td><td>No: pm (**)</td><td>Yes: pg (××)</td><td>No: p1 (o)</td></tr>
</table>

Group labeling algorithm



IMAGE (DATA) -> GROUP LABEL IS BASED ON TESTING THE BEHAVIOR OF GEOMETRIC FEATURES BY INDIVIDUAL OPERATIONS

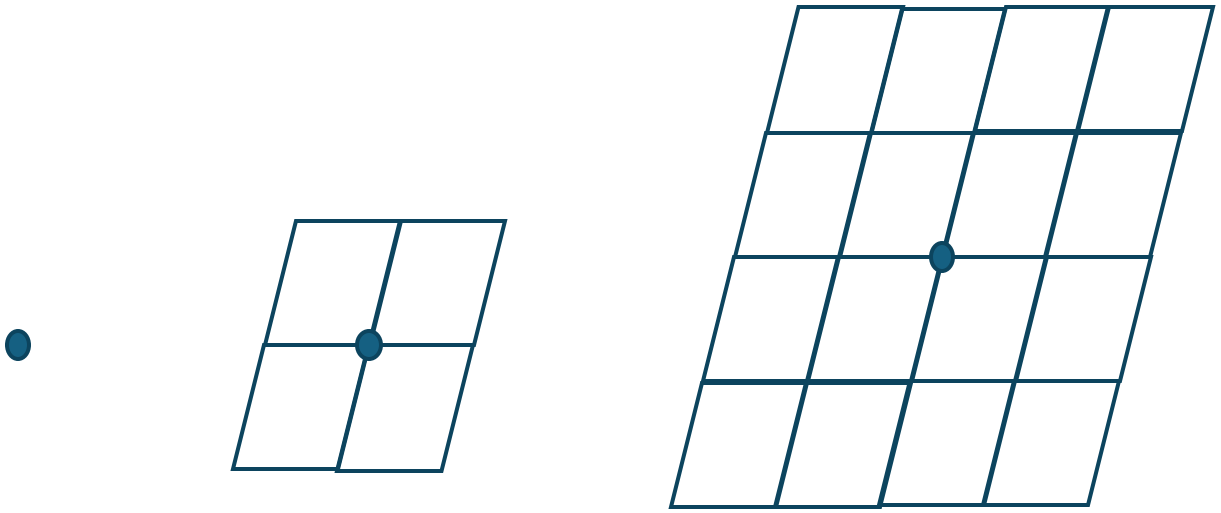


VERY EXPENSIVE!



OUR IDEA IS TO CREATE AN "EQUIVALENT" REPRESENTATION OF THE CRYSTAL THAT IS SIMPLER TO CODE, BUT RETAINS THE SYMMETRY GROUP!

Growth polynomials for p1



$$f_0(n) = 1 \cdot (2n)^2 + 2(2n) + 1$$

$$f_1(n) = 2 \cdot (2n)^2 + 2(2n)$$

$$f_2(n) = 1 \cdot (2n)^2$$

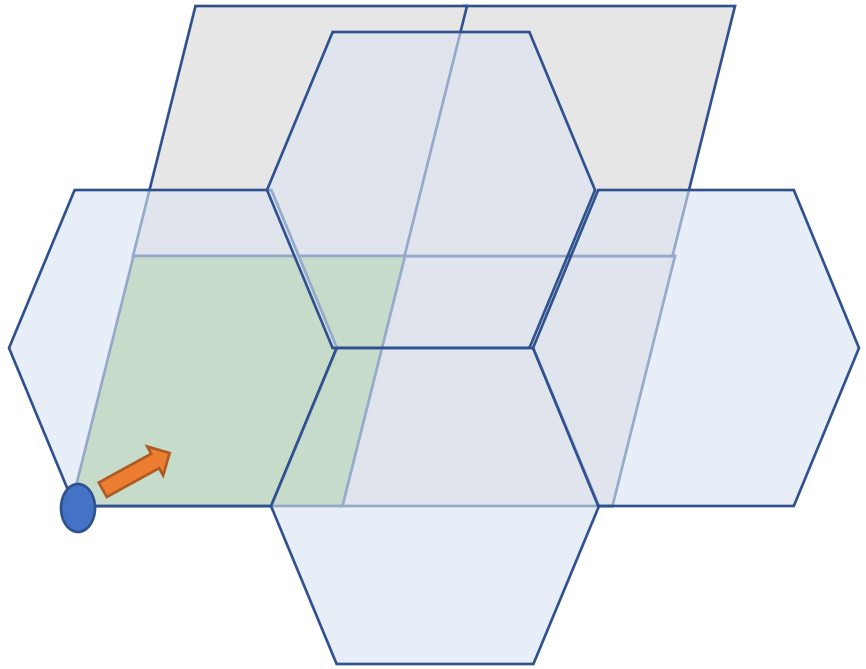
$f_0(n)$ - number of vertices in the distance <= n from the blue dot

$f_1(n)$ - number of edges in the distance <=n from the blue dot

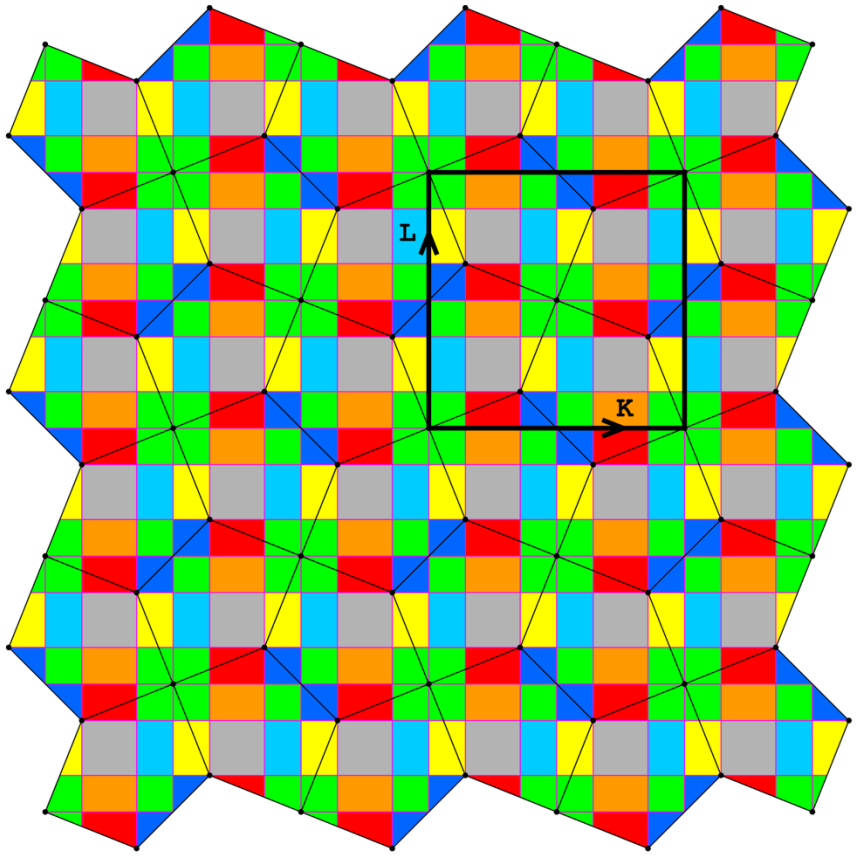
$f_2(n)$ - numer of faces in the distance <=n from the blue dot

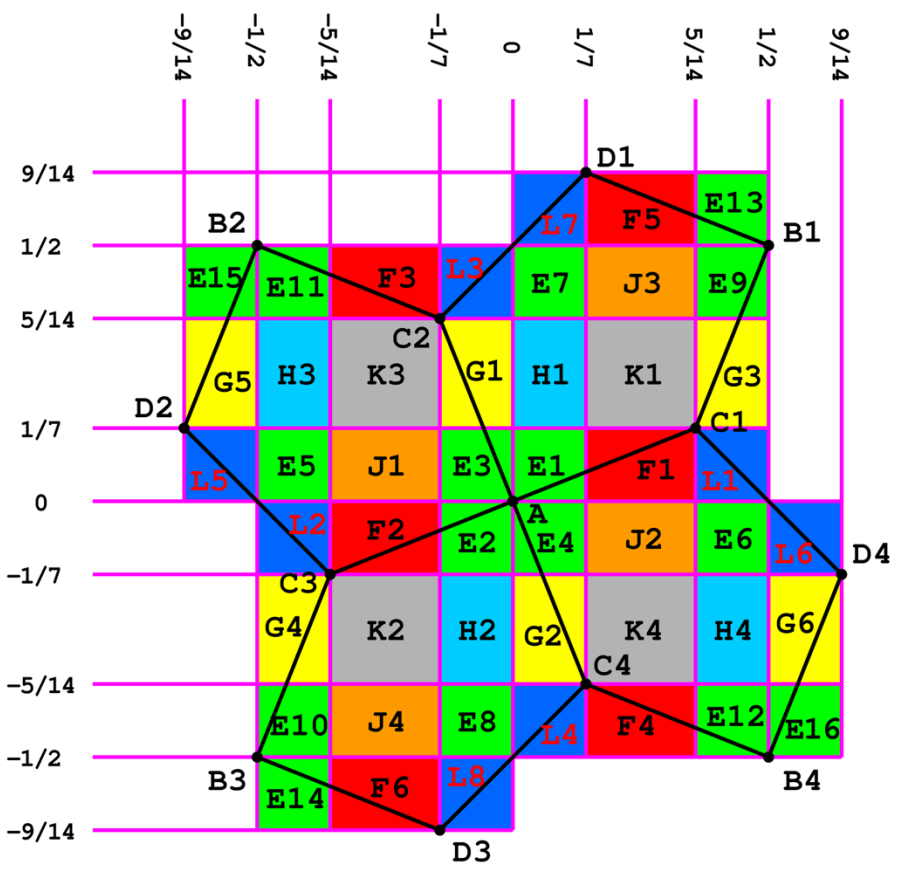
Crystallographic growth function

In our considerations, we discovered so-called crystallographic growth functions, which allow us to encode geometry better than topological ones. Our goal is to describe crystals using these functions!

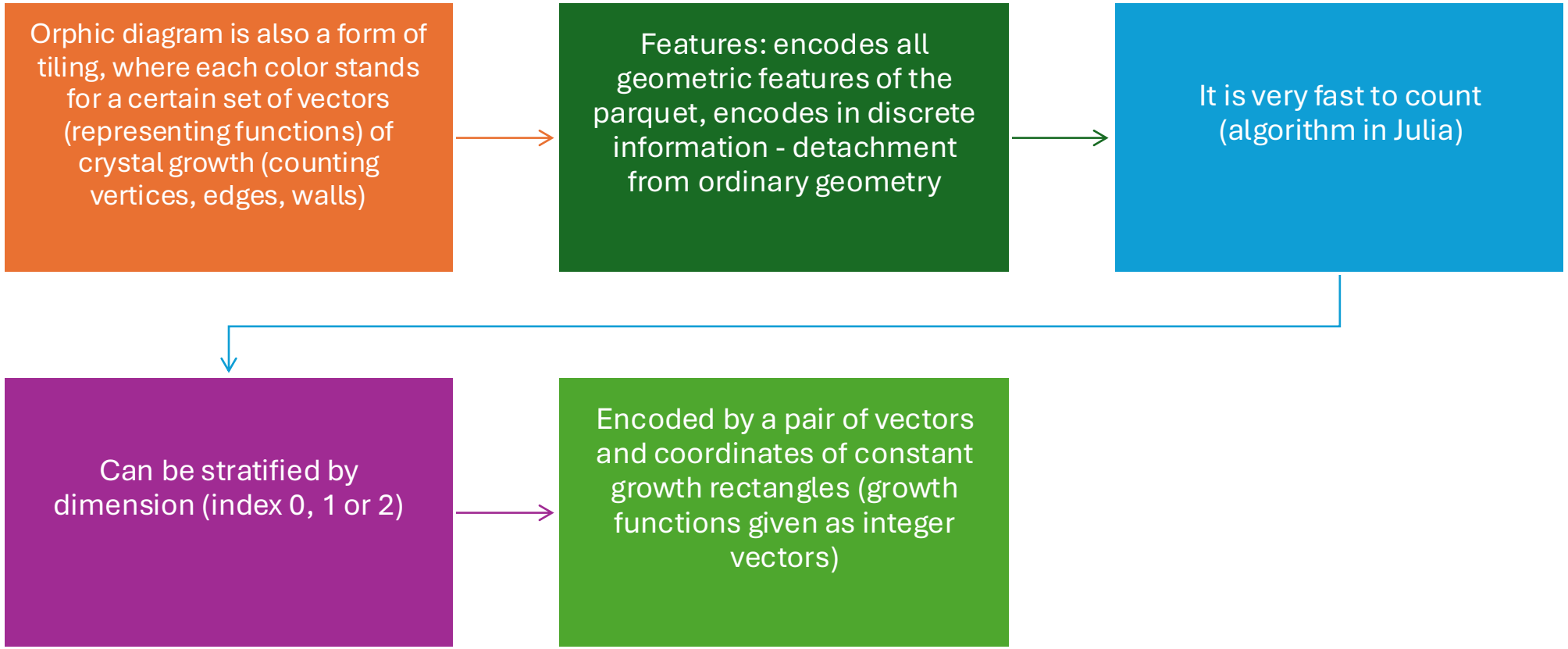


Orphic diagram: 43433 tessellation

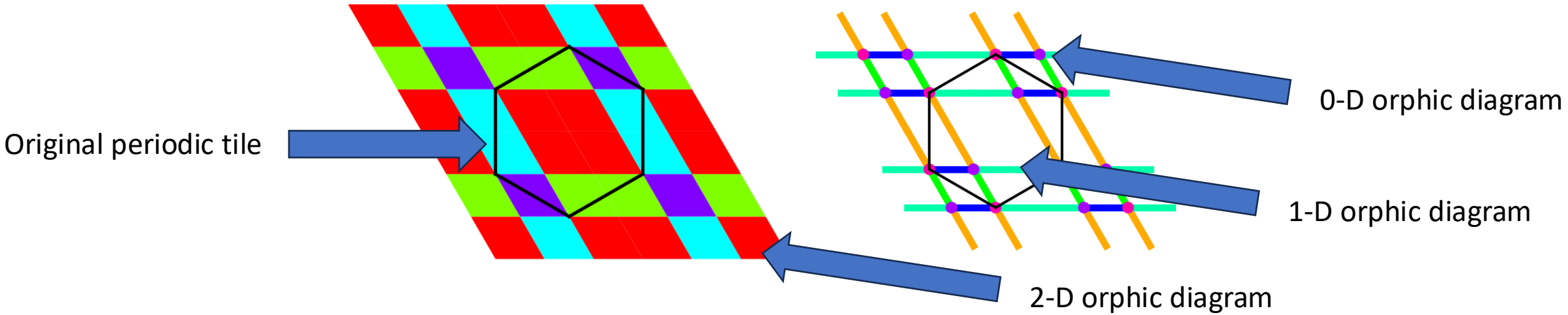




Orphic diagram



Orphic diagrams: 333333 tiling example



- Each colored area denotes a triple of functions (a 12-dimensional vector with integer coefficients.

- The diagram can be defined at the level of diagram vertices (0-dimensional type)
- On the basis of edges (1-dimensional type)
- On the basis of new walls (2-dimensional type)

Machine learning vs. crystallography



We will create classifiers that recognize symmetry groups and pattern structure



Orphic diagrams will serve as input data



Supervised learning will be used

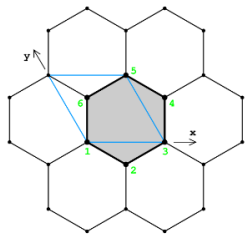


We expect to discover new laws governing the numerical structure of diagrams!

Scheme

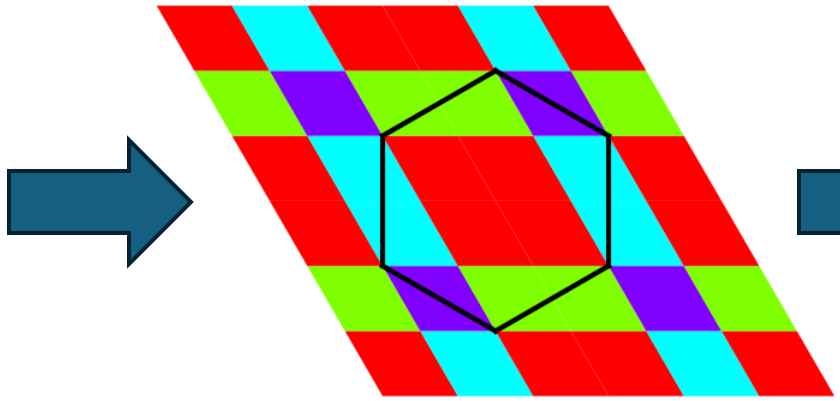
```
6 6 1
  0      0
  1/3   -1/3
  1      0
  4/3    2/3
  1      1
  1/3    2/3
1 2
2 3
3 4
4 5
5 6
6 1
1 2 3 4 5 6
1 0
-1/2 sqrt(3)/2
```

(a)



(b)

Fig. 11. Sample input (a) encoding the 333333 tiling (b). The line 6 6 1 (red) gives V E F, where V is the number of vertices, E is the number of edges, and F is the number of faces. The next 6 (V) lines (green) describe the crystallographic coordinates of the vertices. The next 6 (E) (black) lines describe the connectivity of the vertices (i.e., edges). Finally, the next 1 (F) (red) line(s) describe the faces. The last two (blue) lines specify the translational lattice.



p6mm group, i.e.

- Center of rotation by 1/6 of full angle
- Symmetry axis (m)

Crystal data (optional)

Orphic diagram (input)

Symmetry group - label

Machine learning group types



Using decision tree classifiers, feature engineering, and a hierarchical framework, we have developed a method to classify most of the 17 wallpaper symmetry groups based solely on growth function coefficients.



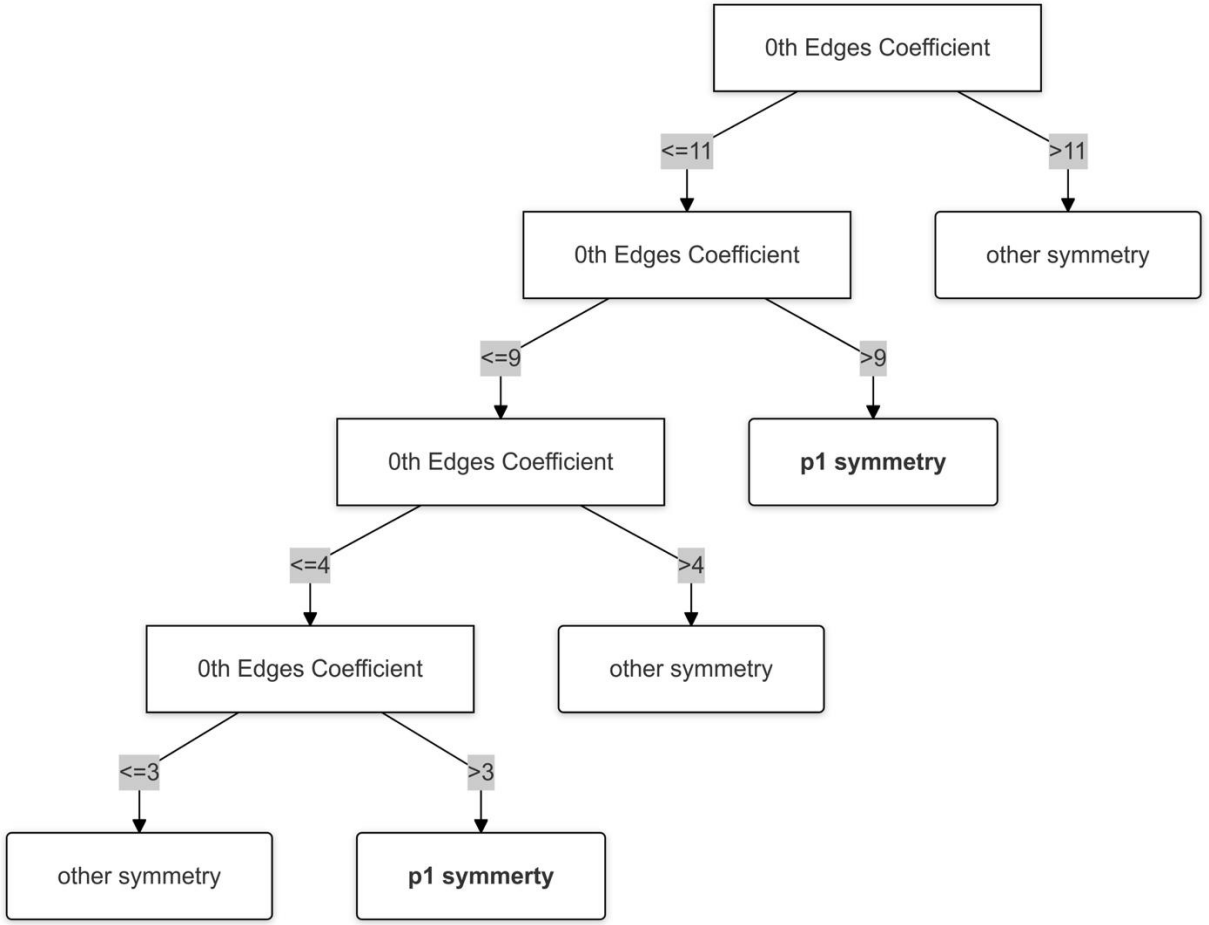
Our approach exploits mathematical properties, particularly divisibility relationships between coefficients, to separate symmetry groups with perfect accuracy.



The hierarchical classification begins with the most general group (p1) and progressively distinguishes groups with increasing symmetry complexity. By analyzing patterns in the coefficients, we identify rules that perfectly separate groups with different rotational, reflective, and glide symmetries.

Machine learning group types

- Our experiments show that different types of symmetry leave distinct mathematical "fingerprints" in the growth function coefficients. For example:
- Rotational symmetry of order 2 can be detected through specific values of C_{00}
- \item Reflection symmetry influences divisibility patterns between C_{10} and C_{00}
- Higher-order rotational symmetries (3, 4, 6) are distinguished by characteristic coefficient values



4.1.1 Separating $p1$ from Other Symmetry Groups

The first stage aimed to separate the $p1$ symmetry group from all other groups. We iteratively tested individual features for their ability to distinguish $p1$. Our algorithm generated two decision trees based on the features $\mathbf{C_{00}}$ (Figure 2) and $\mathbf{C_{10}}$ (Figure 3), which achieved perfect separation. From these, the following rules were identified:

$$
\begin{aligned}
f_0(m,n) &= \mathbf{C_{00}}mn + C_{01}m + C_{02}n + C_{03} \\
f_1(m,n) &= \mathbf{C_{10}}mn + C_{11}m + C_{12}n + C_{13} \\
f_2(m,n) &= \mathbf{C_{20}}mn + C_{21}m + C_{22}n + C_{23}
\end{aligned}
$$

Rule	$\mathbf{C_{00}}$	C_{01}	C_{02}	C_{03}	$\mathbf{C_{10}}$	C_{11}	C_{12}	C_{13}	$\mathbf{C_{20}}$	C_{21}	C_{22}	C_{23}
p_1	$\{4,5\}$											
p_1					$\{4,10,11\}$							

4.1.2 Distinguishing Minimal Rotations $\rho_{\text{rotation}}(s, 2) = 1$ and $\rho_{\text{rotation}}(s, 3) = 1$

At the second hierarchical level, symmetry groups were categorized by their minimal rotation. Groups with $\rho_{\text{rotation}}(s, 2) = 1$ (e.g., $p2, p2gg, p2mg, p2mm$) were compared against those with $\rho_{\text{rotation}}(s, 3) = 1$ (e.g., $p3, p3m1, p31m$). Using all features, we constructed decision trees (Figure 4) that yielded perfect classification. The discovered rules are:

$$
\begin{aligned}
f_0(m, n) &= \mathbf{C_{00}}mn + C_{01}m + C_{02}n + C_{03} \\
f_1(m, n) &= \mathbf{C_{10}}mn + C_{11}m + C_{12}n + C_{13} \\
f_2(m, n) &= \mathbf{C_{20}}mn + C_{21}m + C_{22}n + C_{23}
\end{aligned}
$$

Rule	$\mathbf{C_{00}}$	C_{01}	C_{02}	C_{03}	$\mathbf{C_{10}}$	C_{11}	C_{12}	C_{13}	$\mathbf{C_{20}}$	C_{21}	C_{22}	C_{23}
$\rho_{\text{rotation}}(s, 2)$	$\mathbf{(0, 6\rangle}$											
$\rho_{\text{rotation}}(s, 2)$	$\mathbf{\{9, 10, 11\}}$											
$\rho_{\text{rotation}}(s, 3)$	$\mathbf{(11, \infty)}$											
$\rho_{\text{rotation}}(s, 3)$	$\mathbf{\{7, 8\}}$											

4.1.3 Distinguishing Minimal Rotations $\rho_{\text{rotation}}(s,2)=1$ and $\rho_{\text{rotation}}(s,6)=1$

The final stage examined groups with minimal rotation $\rho_{\text{rotation}}(s,2)=1$ against those with $\rho_{\text{rotation}}(s,6)=1$ (e.g., $p6mm$, $p6$). We tested separability using all features and derived the following rules from the produced tree (Figure 5):

$$
\begin{aligned}
f_0(m,n) &= \mathbf{C_{00}}mn + C_{01}m + C_{02}n + C_{03} \\
f_1(m,n) &= \mathbf{C_{10}}mn + C_{11}m + C_{12}n + C_{13} \\
f_2(m,n) &= \mathbf{C_{20}}mn + C_{21}m + C_{22}n + C_{23}
\end{aligned}
$$

Rule	$\mathbf{C_{00}}$	C_{01}	C_{02}	C_{03}	$\mathbf{C_{10}}$	C_{11}	C_{12}	C_{13}	$\mathbf{C_{20}}$	C_{21}	C_{22}	C_{23}
$\rho_{\text{rotation}}(s,2)$					$\{13,14\}$							
$\rho_{\text{rotation}}(s,2)$	$(4,\infty)$				$(0,12\rangle$				$(0,5\rangle$			
$\rho_{\text{rotation}}(s,2)$	$(0,4\rangle$				$\{5\}$				$(0,5\rangle$			
$\rho_{\text{rotation}}(s,6)$					$(14,\infty)$							
$\rho_{\text{rotation}}(s,6)$					$(0,12\rangle$				$(5,\infty)$			
$\rho_{\text{rotation}}(s,6)$	$(0,4\rangle$				$\langle 6,12\rangle$				$(0,5\rangle$			
$\rho_{\text{rotation}}(s,6)$	$(0,4\rangle$				$(0,4\rangle$				$(0,5\rangle$			

Conclusion

Novel Methodology: Introduces a new approach for classifying 2D symmetry groups using growth polynomial coefficients from crystallographic tiling patterns, enhanced by feature engineering and decision tree classifiers.

Hierarchical Classification: Employs a hierarchical framework that progressively refines classification based on symmetry characteristics, especially rotational symmetries.

Interpretable Rules: Achieves accurate results with explicit, interpretable rules, reducing the need for manual analysis and facilitating deeper understanding of symmetry group structures.

Future Directions: Suggests using symbolic regression to uncover precise boundary functions and emphasizes the need for larger, more diverse datasets to improve model robustness and explore more complex techniques.



Thank you!